



AMERICAN UNIVERSITY OF BEIRUT

USE OF FINE RECYCLED CONCRETE AGGREGATES IN  
ASPHALT MIXTURES

by  
DIMA ZUHAIR AL HASSANIEH

A thesis  
submitted in partial fulfillment of the requirements  
for the degree of Master of Engineering  
to the Department of Civil and Environmental Engineering  
of the Faculty of Engineering and Architecture  
at the American University of Beirut

Beirut, Lebanon  
June 2014

AMERICAN UNIVERSITY OF BEIRUT

USE OF FINE RECYCLED CONCRETE AGGREGATES IN  
ASPHALT MIXTURES

by  
DIMA ZUHAIR AL HASSANIEH

Approved by:



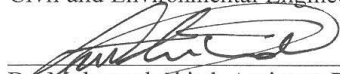
---

Dr. Ghassan Riad Chehab, Associate Professor      Advisor  
Civil and Environmental Engineering Department



---

Dr. George Saad, Assistant Professor      Member of Committee  
Civil and Environmental Engineering Department



---

Dr. Mohamad Abiad, Assistant Professor      Member of Committee  
Nutrition and Food Science Department



---

Dr. Issam Srour, Assistant Professor      Member of Committee  
Engineering Management Program

Date of thesis defense: July 4, 2014

AMERICAN UNIVERSITY OF BEIRUT

THESIS, DISSERTATION, PROJECT RELEASE FORM

Student Name: Al Hassamieh Dima Zuhair  
Last First Middle

Master's Thesis Dissertation       Master's Project       Doctoral

I authorize the American University of Beirut to: (a) reproduce hard or electronic copies of my thesis, dissertation, or project; (b) include such copies in the archives and digital repositories of the University; and (c) make freely available such copies to third parties for research or educational purposes.

I authorize the American University of Beirut, **three years after the date of submitting my thesis, dissertation, or project**, to: (a) reproduce hard or electronic copies of it; (b) include such copies in the archives and digital repositories of the University; and (c) make freely available such copies to third parties for research or educational purposes.

Dima 26/09/2014  
Signature Date

This form is signed when submitting the thesis, dissertation, or project to the University Libraries

## ACKNOWLEDGMENTS

I would like to gratefully and sincerely thank Professor Ghassan Chehab for his guidance, understanding, patience, and help throughout the past two years.

Also, I would like to express my gratitude to Professor George Saad, Professor Mohamad Abiad, and Professor Issam Srour for participating in my thesis committee and for providing me with their helpful guidance and insights.

I would like to express my appreciation to Mr. Helmi El-Khatib, without his help, never ending teaching, and guidance I wouldn't have reached this point.

I would like to thank Mr. Jihad Jammal for his continuous help in the lab work and for his valuable friendship. I would also like to thank the undergraduate students working in the Pavement lab. Staff and graduate students at the Central Research Science Laboratory, Rheology lab, and the Structures and Materials lab, are highly appreciated especially Abdel Rahman Sheikh and Bashir Asyala.

In addition, I would like to thank my friends for their help, support, and encouragement.

Thanks for Mr. Hussein Kassem for being my friend, partner and for always going the extra mile to help me in my research work.

The encouragement, patience, sacrifices and care of my parents, got me where I am now. Thanks to all their efforts and all their love; for that I will be indebted forever.

# AN ABSTRACT OF THE THESIS OF

Dima Zuhair Al Hassanieh for Master of Engineering  
Major: Materials and Pavement Engineering

Title: Use of Fine Recycled Concrete Aggregates in Asphalt Mixtures

Currently, environmental protection and sustainability have become basic concerns around the world. Many industries, one of which is construction, have set initiatives towards more environmental friendly practices. Lebanon, the scope of this study, is facing a crisis when it comes to construction and demolition waste management and disposal. These wastes are produced either from emergencies as wars and earthquakes or from the development of cities and increase in population. Therefore, viewing construction demolition waste as a resource rather than waste is essential, basically as a construction material where considerable amount can be used in roadway construction activities. The main objective of this research is to evaluate using fine recycled concrete aggregates (RCA) into hot mix asphalt (HMA). The work scope consists of conducting fundamental material property tests for the RCA and the natural aggregates used, conducting mix designs using Marshall mix design and Superpave mix design for a control mix consisting of natural limestone aggregates only and mixes where 10%, 15%, 20%, 30%, and 45% of the fine aggregates are replaced with fine RCA. In addition, the effect of recycled aggregates filler will be studied on the mastic level. Analysis of testing results for Marshall Stability, dynamic modulus, mastic complex modulus, and non-recoverable creep compliance reveal acceptable results for incorporating fine recycled concrete aggregates in HMA up to 20-30%.

# CONTENTS

	Page
ACKNOWLEDGEMENTS.....	v
ABSTRACT.....	vi
LIST OF ILLUSTRATIONS.....	x
LIST OF TABLES.....	xii

Chapter	Page
1.INTRODUCTION.....	1
1.1. Problem Statement.....	1
1.2. Research Needs .....	2
1.3. Research Objectives and Significance.....	3
2. LITERATURE REVIEW.....	4
2.1 Use of CDW in the Construction Industry.....	4
2.2 Use of RCA in Construction Materials.....	6
2.3 Moisture Sensitivity in HMA.....	9
2.3.1 Adhesion Theories .....	12
2.3.2 Cohesion Theories .....	12
3. PROPOSED METHODOLOGY AND SCOPE OF RESEARCH.....	14

3.1 Materials used .....	14
3.1.1 Aggregates.....	14
3.1.2 Asphalt binder .....	15
3.2 Bailey Method.....	15
3.2.1 Optimum Aggregate Gradation .....	15
3.3 Marshall and Superpave Mix Design .....	20
3.3.1 Optimum Asphalt Content using Marshall Mix Design .....	21
3.3.2 Testing of Marshall Specimens .....	22
3.3.3 Testing of Superpave Specimens.....	26
3.4 Mastic Testing.....	33
<b>4. RESULTS AND ANALYSIS.....</b>	<b>35</b>
4.1 Material Properties .....	36
4.1.1 Aggregates.....	36
4.1.2 Asphalt Binder.....	40
4.2 Marshal Mix Design.....	41
4.3 Superpave Mix Design .....	49
4.3.1 Optimum Asphalt Content Validation .....	49
4.3.2 Superpave Optimum Asphalt Content .....	50
4.3.3 Dynamic Modulus .....	52
4.4 Mastic Testing.....	62
4.4.1 Viscosity.....	63
4.4.2 Complex Shear Modulus and Phase angle .....	65
4.4.3 Multiple Stress Creep and Recovery.....	68
<b>5. CONCLUSIONS AND FUTURE WORK.....</b>	<b>70</b>



5.1 Conclusions.....	70
5.2 Future Work.....	71
REFERENCES.....	72
APPENDIX-A.....	77
APPENDIX-B.....	82
APPENDIX-C.....	92

# ILLUSTRATIONS

Figure		Page
1	Two Possible moisture damage mechanisms (After Caro, 2009) .....	11
2	Flow Chart showing the separation of an aggregate blend into coarse and fine according to Bailey method .....	17
3	Aggregate gradation used in the mix design .....	19
4	Complex modulus graphical representation (After Chehab, 2002).....	29
5	SEM images of (a) natural aggregates and (b) recycled aggregates .....	38
6	SEM images of #100(0.15mm) size(a)natural aggregate and (b) recycled aggregates .....	38
7	SEM images of #200(0.075mm) size(a)natural aggregate and(b) recycled aggregates .....	39
8	SEM image of natural pan at 2 um.....	39
9	SEM image of Recycled pan at 20um .....	40
10	Binder $G^*/\sin(\gamma)$ values for different tested temperatures.....	41
11	AV% versus AC% for the six mixes .....	42
12	VMA versus AC% for the six mixes .....	44
13	VFA versus AC% for the six mixes .....	46
14	Stability versus AC% for the five mixes .....	47
15	Flow versus AC% for the five mixes.....	48
16	n-value versus %RCA in the mi .....	52
17	Master curve for natural mixes at reference temperature - three replicates.....	53
18	E* master curve for mixes with 10% RCA at reference temperature - three replicates .....	54
19	E* master curve for mixes with 15% RCA at reference temperature - three replicates .....	55
20	E* master curve for mixes with 20% RCA at reference temperature - three replicates .....	56
21	E* master curve for mixes with 30% RCA at reference temperature - three replicates .....	57

22	Average dynamic modulus mastercurves for mixes with different % fine RCA.....	58
23	Phase angle master curves for mixes with different % of fine RCA.....	58
24	Comparison of mixes with fine RCA to the control mix.....	59
25	Viscosity values for each of the six mastics prepared.....	65
26	$G^*/\sin\delta$ at different temperatures for the 5 mastics prepared.....	66
27	Jnr results for the five mastics.....	68

# TABLES

Table	Page
1 Chosen UW as a percent of LUW and the corresponding mix performance.....	18
2 Recommended Ranges of Aggregate Ratios.....	19
3 Three calculated parameters and their corresponding ranges. ....	20
4 Marshal Design criteria.....	25
5 Minimum percent voids in mineral aggregates.....	25
6 Superpave design requirements.....	27
7 Loads used in the dynamic modulus test for each temperature frequency combination.....	32
8 Sample to be tested for the mastic study.....	34
9 Specific gravity and absorption of RCA and natural aggregates .....	37
10 Surface area of recycled and natural filler .....	37
11 Compressive strength of recycled and natural aggregates.....	37
12 Results of tests performed on asphalt binder .....	40
13 Optimum asphalt content for each of the 6 mixes.....	43
14 Volume of effective binder for each asphalt content for each of the five mixes .....	45
15 IDT results, average Air voids of the tested specimens, & the corresponding TSR.	49
16 Results of Superpave samples compacted at optimum AC% used from Marshall ...	50
17 Results of Superpave samples compacted at calculated AC% .....	51
18 Results of Superpave samples compacted to Nmax .....	51
19 Ranking of the mixes based on the rutting stiffness factor.....	61
20 Ranking of the mixes based on the fatigue stiffness factor .....	62

I dedicate this work to my late grandmother, Nadima

# CHAPTER 1

## INTRODUCTION

### **1.1. Problem Statement**

Natural resources' shortage and waste management are two interrelated concerns. Aiming at a green sustainable construction industry, the use of construction waste material as a recycled material in new construction applications serves a dual purpose. Looking into waste material as a resource rather than just waste, researchers are incorporating the use of waste generated in construction and demolition (CDW) into engineering applications as a means of sustainable development. Thus the construction industry, being the main contributor for the CDW generated, has to be directed towards green oriented practices that help in protecting the environment, solving problems arising in landfills, and minimizing resources' consumption. According to Srour et al. (2013), the Lebanese construction industry is considered as one of the highest growing sectors fueled by the rapid economic and population growth occurring in a country of limited area. This has stipulated the need to demolish old, outdated, and mostly small buildings and replace them with modern and high occupancy facilities. That resulted in the generation of high amounts of CDW estimated to be about one million ton for the city of Beirut alone in 2009 and 2010. Another significant resource of solid waste in Lebanon is from the destruction resulted from 2006 and 2007 wars. In 2006, the amount of rubble generated was estimated to be about 5.6 million cubic meters, which constitutes around 23% of the total volume of waste generated in Lebanon per year (Rebuild Lebanon, 2008). The concern was to remove the waste quickly so as to allow the reconstruction processes to start, therefore the main dumping sites were empty lots,

valleys, and ravines (Rebuild Lebanon, 2008). According to United Nations Development Programme (2008), the main composition of the generated waste is concrete which constitutes 50% - 70% of the total waste generated. Thus, the use of CDW as a replacing material for natural aggregates might be a feasible investment.

## **1.2. Research Needs**

Recycled aggregate (RA) is defined in BS 8500-1 (2006) as the generic term for aggregate resulting from the reprocessing of inorganic material previously used in construction. The first ASTM standard for concrete aggregates (C 33) published in 1985 stated that coarse aggregates consist of gravel, crushed gravel, crushed stone, air cooled blast furnace slag or **crushed hydraulic cement concrete**. Although ASTM states that crushed hydraulic cement concrete has been used as aggregates with satisfactory results, it may require some additional precautions. Due to the high contaminants present in construction and demolition waste, looking into demolition waste coming from concrete only was considered in this study specifically the fine portion of the recycled concrete aggregates. Several researchers have investigated the use of recycled aggregates in concrete. Most research focused on the use of coarse recycled aggregates in concrete and reached satisfactory results when it comes to strength (Uche, 2008; Evangelista et. al, 2007; Nixon, 1978; Corinaldesi, 2004; Neville, 1995). In addition, studies also showed the use of coarse recycled aggregates in HMA with few studies incorporating the use of fine recycled concrete (Rosario et. al, 2011; Paravithana et.al, 2006; Zhu et.al, 2012; Mills-Beale, 2010; Perez et.al, 2012; Arabani et. al, 2012; Cho et.al, 2010).

Lebanon faces a problem when it comes to fine aggregates where huge amounts are being imported from Egypt. Fine recycled concrete aggregates have not been extensively investigated in literature thus focusing on using fine recycled aggregates

might be a possible solution worth investigating. This research will investigate the use of fine recycled concrete aggregates obtained from the selective demolition of concrete structural members in HMA.

### **1.3. Research Objectives and Significance**

Viewing CDW as a source of material considerable amounts can be used in roadway construction activities. The objective of this research is to evaluate using **fine** recycled concrete aggregates (RCA) in HMA. The study investigates the properties of HMA mixes with different percentage of RCA using Marshall Mix Design. The study further investigates these mixes using Superpave Mix Design. Moreover, the Dynamic Modulus master curve is determined in order to characterize the material behavior under various loading and temperature conditions. Furthermore, the fundamental material properties for both types of aggregates, the asphalt binder and the mastic (asphalt + filler material) is determined in order to explain the macro scale behavior of the asphalt mixtures.



## CHAPTER 2

### LITERATURE REVIEW

“Sustainability is to provide the demands of the present generation without compromising the needs of the future generations” (Burton, 1987). By the same token, the Union of Conservation Scientists (IUCN), United Nations Environment Programme (UNEP) and World Wide Fund for Nature (WWFN) define sustainability as “improving the quality of life while living within the carrying capacity of the Earth’s supporting eco-systems” (Evans, 2014) Therefore, looking at the resources that nature provides, one must think of ways to ensure that these resources do not deplete. Hence, the need to consider aspects such as recycling is necessary especially in the construction sector. The consequent section presents the use of CDW in several countries, the standards that have been issued for their use and the use of RCA in construction materials (concrete and HMA). The section ends with an overview of the failure mechanism of HMA due to moisture.

#### **2.1 Use of CDW in the Construction Industry**

The construction industry has become the greatest contributor of waste (Vazquez, 2013). According to the European statistical office, 48% of the waste produced comes from the construction and demolition sectors. Out of this type of waste, three main components are dominant; concrete, masonry rubble, and stone (Vazquez, 2013). Fueled by several economic drivers, the use of construction demolition waste in construction applications has increased. This is due to the increase in landfill costs that recycling CDW has become a more economical option (John and Angulo, 2013). A report by FHWA (2004) indicated that a one-lane mile of 10 inch thick Portland Cement

Concrete (PCC) pavement needs approximately 3,000 tons of coarse and fine aggregates; that same mile at the end of its service life produces 4,000 ton of RCA (Wattenberg-Komas and Stroup-Gardiner, 2013). Thus, several countries have started to issue standards and recommendations for the use of RCA. In Canada, the C-2000 Green Building Standards set the goal of making recyclable material up to 75% (Mishulovich, 2003). In Belgium, the specifications indicate that recycled aggregates can be added to a maximum of 20% by volume of the total coarse aggregates (Vrijders and Desmyter, 2013). In Italy, the percentage of use of recycled aggregates from concrete goes up to 60% replacement of natural aggregates (Bassan and Quattrone, 2013). In addition, Germany recommends a maximum use of 50% of RCA as a replacement of coarse aggregate.

According to FHWA, in the US, 41 out of 50 states recycle old concrete to be used as aggregates; 38 of which use the aggregates for base/sub-base while the rest use the RCA in concrete (FHWA, 2004). Lebanon, on the other hand, still lacks any figures for the amount of demolition waste generated (Srour et al., 2012) and evidently lacks any recommendations on the use of RCA. According to Srour et al. (2013), the construction boost that is present in Lebanon is increasing significantly the amount of demolition waste generated from demolishing old/outdated building and the illegal dumping of such waste (Srour et al., 2013). In addition to the demolition waste, Lebanon faces another type of demolition waste that is the “emergency waste” generating from wars. In 2006 and 2007 wars a total of 6.6 million m<sup>3</sup> of rubble was generated (UNRWA, 2008). Moreover, the Lebanese quarries generate 3 million m<sup>3</sup> of aggregates while the demand for construction is 3.7 million m<sup>3</sup> (Srour et al., 2012). Thus, using RCA as a construction material is the solution for two major problems.

## **2.2 Use of RCA in Construction Materials**

The use of RCA has been an interest for many researchers to ensure sustainable development and environmental welfare in the construction industry. However, RCA's performance is highly dependent on the source of the demolition. One of the first investigations of RCA in concrete was in 1978; Nixon stated that the use of uncontaminated coarse recycled aggregates decreased the compressive strength of concrete slightly. In addition, Nixon stated that the weakest link was the mortar adhering to the aggregates (Nixon, 1978). Moreover, the freeze thaw resistance increased due to the presence of highly porous frost susceptible aggregates. Since then, several researchers investigated the use of coarse recycled aggregates. ACI committee-555 (2001) defined the water to cement ratio to be the most critical part of controlling the strength of a concrete mix having recycled aggregates. To produce mixes with similar workability additional 5% water was found to be required for a mix with coarse RCA while that percent increased to 15% when using both fine and coarse recycled aggregates (ACI-555, 2001). Moreover, a combination of RCA with natural virgin coarse aggregates with percentage replacement of 50% or less provides concrete suitable for structural work (Uche, 2008). In addition, Anderson et al. stated that, when using coarse and fine RCA, the compressive strength is 15% to 40% less than the conventional concrete (Anderson et. al, 2009). ACI-555 states that the fine recycled aggregates tend to be more angular than fine natural aggregates and more water absorbing. This higher water absorption is due to the presence of cement mortar on the aggregates. These two properties tend to make the produced concrete mixes prone to less bleeding (ACI-555, 2001). According to Neville (1995) after the mortar (cement and water) is introduced in the mixer, the water absorption of the recycled aggregates decreases because the binder acts as a sealant to the pores. One of the major problems

presented with the use of recycled aggregates is the presence of deleterious materials such as plasters, clay lumps, asphalt, plastics, paints, paper, and wood. ACI-555 recommends a maximum allowable amount of deleterious materials of 10 Kg/m<sup>3</sup> in coarse and fine aggregates respectively. Furthermore, Nixon stated that the use of fine RCA decreased the workability of the mix dramatically while having no effect on the compressive strength (Nixon, 1978). Another study indicated that the use of fine RCA in mortar showed good bond strength (Corinaldesi, 2004). Moreover, the use of fine RCA was investigated for replacement up to 30% in concrete mixes (Evangelista et. al, 2007). The compressive strength did not seem to be affected by the different percentage replacement of the natural aggregates. However, the tensile splitting and the modulus of elasticity decreased as the percentage of fine recycled aggregates increased although still acceptable (Evangelista et. al, 2007).

As used in concrete, several studies have been conducted to evaluate the incorporation of RCA in pavement construction applications. A research done by Leite et al. (2011) showed that RCA may be utilized as coarse base and sub-base layers for low-volume roads. It showed that the resilient modulus of RCA aggregates is similar to that of a well graded crushed natural stone. It pointed out that the grain size distribution changes fairly as the compaction energy applied increases. Thus, it is required to compact layers of RCA using proper compaction energy and to control it after the compaction process due to its breakage potential. A study by Rosario et al. (2011) examined the use of CDW having only 75% concrete, 20% asphalt, and 5% ceramic material without any other impurity as a base pavement layer. The performance of CDW was the same as natural quarry aggregates. The bearing capacity of the CDW material was found to be satisfactory as long as more amounts of water were added

while spreading and before compaction. In addition, it was found that as successive pavement layer are applied, the load-bearing capacity of the base improved.

A study done by Parनावithana et al. (2006) to examine the use of coarse RCA in HMA indicated that the bulk density, voids in mineral aggregates (VMA), voids filled with asphalt (VFA) and film thickness were lowered in mixes with RCA compared to control mixes where the natural aggregates used were basalt. It also showed that the resilient modulus of HMA with RCA is decreased with a **higher stripping potential** were great variation in strength between dry and wet conditions was observed. Referring to Zhu et al. (2012), recycled concrete aggregates possess potential problems of low strength, low specific gravity, high absorption, and **poor moisture resistance** of asphalt mixtures. Replacing the whole aggregate skeleton or only its coarse proportion with RCA of same size in HMA, leads to a higher optimum asphalt content (AC), lower Marshall stability, and lower indirect tensile strength (IDT) than mixes with only natural aggregates. Also, it affects the moisture resistance and the flexibility of asphalt mixtures at low temperature. However, the study indicated that treating the coarse recycled aggregates with a liquid silicone resin improves their properties effectively. In addition, a research study done by Mills-Beale (2010) showed that it is acceptable to use up to 75% RCA replacement of natural aggregates without causing a problem in permanent deformation. Moreover, the study indicated the increase of moisture susceptibility as RCA increased. However, the study showed that RCA is capable of serving as a useful replacement in HMA roadways when the traffic is minimal where it possesses significant energy savings during the compaction process. Perez et al. (2012) researched the effect of using RA as coarse aggregates with 3 different percentages with two different types of natural aggregates. The results showed that the HMA containing RA showed an increase in indirect tensile strength in the dry

state however, a drop in tensile strength ratio. Perez et al. contributed this to the stripping behavior of the HMA with RA which can be linked to the poor adhesion of the RA and their high absorption. The study recommended that the fine fraction not be used due to the high impurities, and that the laboratory tests should provide sufficient time to allow the recycled aggregates to absorb the binder effectively. Perez et al. (2011) showed in another study conducted on the use of coarse recycled concrete aggregates with two types of filler: cement and lime, that using RCA in HMA provided a good resistance to permanent deformation. However, the mixes are highly susceptible to the **water action** therefore the use of anti-stripping agents and pretreatments of the RA to remove any impurities in the coarse RA is needed to improve the durability. Arabani et al. (2012) studied the effect of using recycled aggregate as fine and coarse aggregates along with steel slag. The mixes with only fine recycled aggregates replacement showed a decrease in permanent deformation, a greater fatigue life, and a 44% greater resilient modulus compared to control mixes. Cho et al. (2010), concluded from a study about the use of RCA in HMA, that mixes with 100% fine RCA replacement gave the highest rutting resistance along with higher deformation strength. This was attributed to the effect of the aggregate friction caused by the fine RCA that increase the strength of the coarse aggregate skeleton. In addition, the study indicates that the binding strength of the asphalt binder has a higher effect on the tensile strength of the mix rather than the aggregate type.

### **2.3 Moisture Sensitivity in HMA**

As previously mentioned several studies have indicated the problem with using RCA, specifically fine RCA, as being the low moisture resistance of these aggregates. Therefore, in order to understand the mechanism behind the low resistance of these

aggregates, the need to understand the failure mechanism of HMA due to moisture is required. Moisture damage is a detrimental effect caused by the presence of moisture in asphalt pavement. This moisture causes the degradation of the pavement along with the development of other distresses (Caro, 2009). Kiggufu and Roberts (1988) provide a definition of moisture damage as “the progressive functional deterioration of a pavement mixture by loss of the adhesive bond between the asphalt cement and the aggregate surface and/or loss of the cohesive resistance within the asphalt cement principally from the action of water”. Thus two types of failure mechanisms can occur. According to Caro (2009), adhesive bonds play a more important role in moisture damage presented as the stripping potential of the binder from the aggregates. According to Little and Jones (2003), the literature refers to five different stripping mechanics: detachment, displacement, spontaneous emulsification, pore pressure and hydraulic scour.

Detachment: is the separation of an asphalt film from an aggregate surface by thin film of water without a clear break in the film (Majidzadeh and Brovold, 1968). This bond is dependent on the ability of the asphalt to wet the aggregate and this is dependent on the free surface energy. According to Little and Jones (2003) and based on surface energy measurements, the aggregate surface has a strong affinity for water over asphalt

Displacement: is the displacement of the asphalt film from the aggregate due to the asphalt film breakage. The breakage can be caused by film breakage at sharp aggregate edges or incomplete coating of the aggregates (Little and Jones, 2003).

Spontaneous Emulsification: is “an inverted emulsion of water droplets in asphalt cement” (Little and Jones, 2003). According to Fromm (1974), once the emulsion forms it can easily break the adhesive bond.

Pore Pressure: is the buildup in the pore pressure of the entrapped water that leads to distresses (Little and Jones, 2003). The repeated traffic load will worsen the damage caused by pore pressure due to the growth of micro cracks in the asphalt mastic causing cohesive and adhesive failures (Little and Jones, 2003). However, for this mechanism to occur, researchers suggested the presence of a pessimum air void size where above which the water reaches the material and easily drains out of it because the air voids are interconnected. Below which the infiltration is low and the air voids are disconnected. Thus at this range of pessimum air voids the water gets entrapped favoring the moisture damage to occur (Terrel and Al-Swailmi, 1994; Caro, 2009).

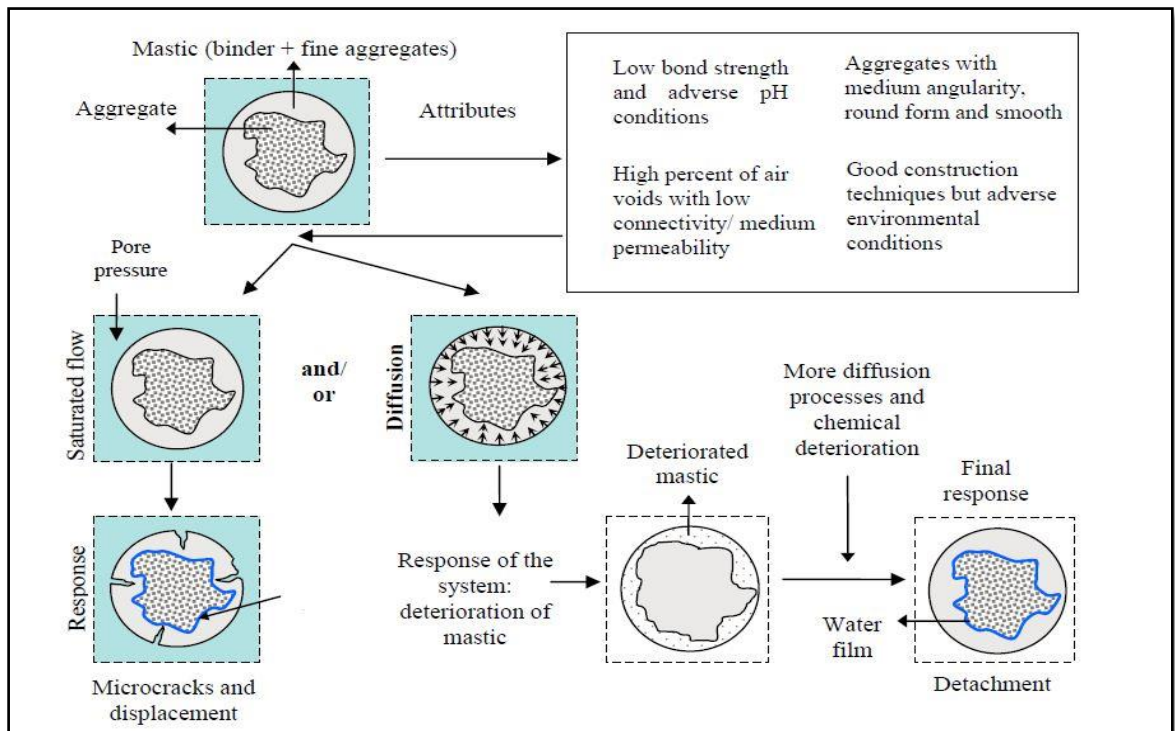


Figure 1 Two Possible moisture damage mechanisms (After Caro, 2009)



Hydraulic Scour: this occurs at the surface of the asphalt due to the action of the tire that causes the water to be infiltrate into the pavement (Caro, 2009)

### ***2.3.1 Adhesion Theories***

Four main theories describe the adhesion between asphalt and aggregates (Terrel and Shute, 1989); chemical reaction, surface energy, molecular orientation, and mechanical adhesion. These are affected by several factors: surface tension of the asphalt cement and aggregate, chemical composition of the asphalt and the aggregates, asphalt viscosity, surface texture of the aggregate, aggregate porosity, aggregate cleanliness, and aggregate moisture content and temperature at the time of mixing (Terrel and Shute, 1989).

### ***2.3.2 Cohesion Theories***

Cohesion is primarily influenced by the rheology of the filled binder (Little and Jones, 2003). According to Caro (2009), the cohesive strength is controlled by the combination and interaction of the asphalt cement and the mineral filler. Kim et al. (2002) showed that the resistance of mastic (asphalt binder and filler passing sieve # 200) to micro cracks is highly dependent on the dispersion of the mineral filler. The study indicated that the type and amount of filler when properly chosen can withstand more damage (Kim et al. 2002). Therefore, the type of filler can influence the type of failure to occur (Caro, 2009). Terrel and Al-Swailmi indicated that water weakens the cohesive strength of the mastic due to moisture saturation and void swelling.

In brief, researchers have investigated the use of fine RCA in concrete and HMA. The results obtained indicated that using fine RCA in concrete provided similar compressive strength, good bond strength and acceptable tensile splitting and modulus

of elasticity. On the other hand, more researchers focused on the use of either coarse RCA or total RCA replacement in HMA. Therefore, the literature still lacks data on the use of **fine recycled aggregates** obtained from **selective demolition** of concrete structural members. In addition, using demolition waste instead of natural aggregates in Lebanon would provide a sustainable approach in the construction industry.

## CHAPTER 3

### PROPOSED METHODOLOGY AND SCOPE OF RESEARCH

The following sections present the materials used for conducting this study, an explanation of the Bailey method to obtain an optimum aggregate gradation, the Marshal and Superpave Asphalt Mix design methods and the corresponding testing to be conducted.

#### **3.1 Materials used**

##### ***3.1.1 Aggregates***

The natural aggregates used in the asphalt mixtures consist of limestone from West Bekaa, Lebanon, and are representative of what is typically used in roadway projects in Lebanon. The recycled concrete aggregates were obtained by crushing and sizing bulks of demolished Portland cement concrete taken from a 50 year-old demolished building in Beirut.

The first phase of the experimental program consists of determining the physical properties of the natural and recycled aggregates used. The bulk specific gravity of the aggregate,  $G_{sb}$ , and the absorption are required for volumetric calculation of compacted HMA. Testing is done according to ASTM C127-12 and C128-12 respectively. The sand equivalent test is also done for fine aggregates according to ASTM D2419-09. Since the filler material acts as an extender of the binder, its properties are studied on the micro scale using a Scanning Electron microscopy to evaluate the difference in surface texture between the natural and recycled filler. The work also includes using

BET analyzer (Brunauer–Emmett–Teller theory) to determine the surface area of fillers. In addition, the compressive strength of the natural limestone rock and the recycled concrete aggregates were determined. The samples prepared were sawed to get a 10cm and 5cm sided cube for the RCA and natural limestone respectively.

### ***3.1.2 Asphalt binder***

The asphalt binder was obtained from ARACO, a local HMA plant. It is unmodified Pen 60/70 asphalt which is specified for use in all mixtures and regions in Lebanon. The mixing and compaction temperatures used were 165°C and 135°C based on the suppliers' recommendations. Asphalt binder properties are studied by conducting Ductility, Penetration, and Softening Point tests according to ASTM D 113-07, ASTM 5-06, and ASTM 36/D36M-12 respectively which are adopted by the penetration grading system. In addition, the binder is characterized using Dynamic Shear Rheometer according to ASTM D7175-08. Only the high performance grade (PG) of the binder was obtained were the complex shear modulus ( $G^*$ ) and the phase angle ( $\gamma$ ) were determined. Based on Superpave the binder is tested at several grading temperatures, the first value of  $\frac{G^*}{\sin(\gamma)} \geq 1$  at 10 rad/sec indicates the high PG grade of the binder. Moreover, the non-recoverable strain calculated from the multiple stress creep and recovery test according to ASTM D7405.

## **3.2 Bailey Method**

### ***3.2.1 Optimum Aggregate Gradation***

The Bailey Method is used in order to determine the optimal aggregate gradation when using several stockpiles. This method redefines the meaning of coarse and fine aggregates. Using the Bailey method, coarse aggregates are large aggregates that, when

placed in a unit volume, create voids. While fine aggregates, are those that can fill the voids created by the coarse aggregates in the mixture. This method relates the division of the aggregates to the nominal maximum particle size used.

### 3.2.1.1 Division of Aggregates

In order to separate between the fine and coarse aggregates, the Bailey method requires the determination of the Nominal Maximum Particle Size (NMPS). The sieve that separates the aggregate into coarse and fine is defined as the primary control sieve (PCS) and it is determined by equation (1).

$$PCS = NMPS * 0.22 \quad (1)$$

where PCS : Primary control sieve , and NMPS :  
Nominal Maximum Particle size

The 0.22 multiplier is an average value that is determined by the Bailey method after the analysis of two and three dimensional analysis of aggregate packing using different aggregate shapes. Therefore, the division is dependent on the NMPS of the aggregate stockpile and not on a specific sieve size as defined by American Society for Testing and Materials.

The Bailey method further separates aggregates into fine and coarse. As such, the method defines another three sieves determined by the following equations:

1. Secondary Control Sieve (SCS) = PCS \* 0.22
2. Tertiary Control Sieve (TCS) = SCS\*0.22
3. Half Sieve = 0.5\* NMPS

As shown in Figure 2, each of the previously defined sieves separates the aggregates further.

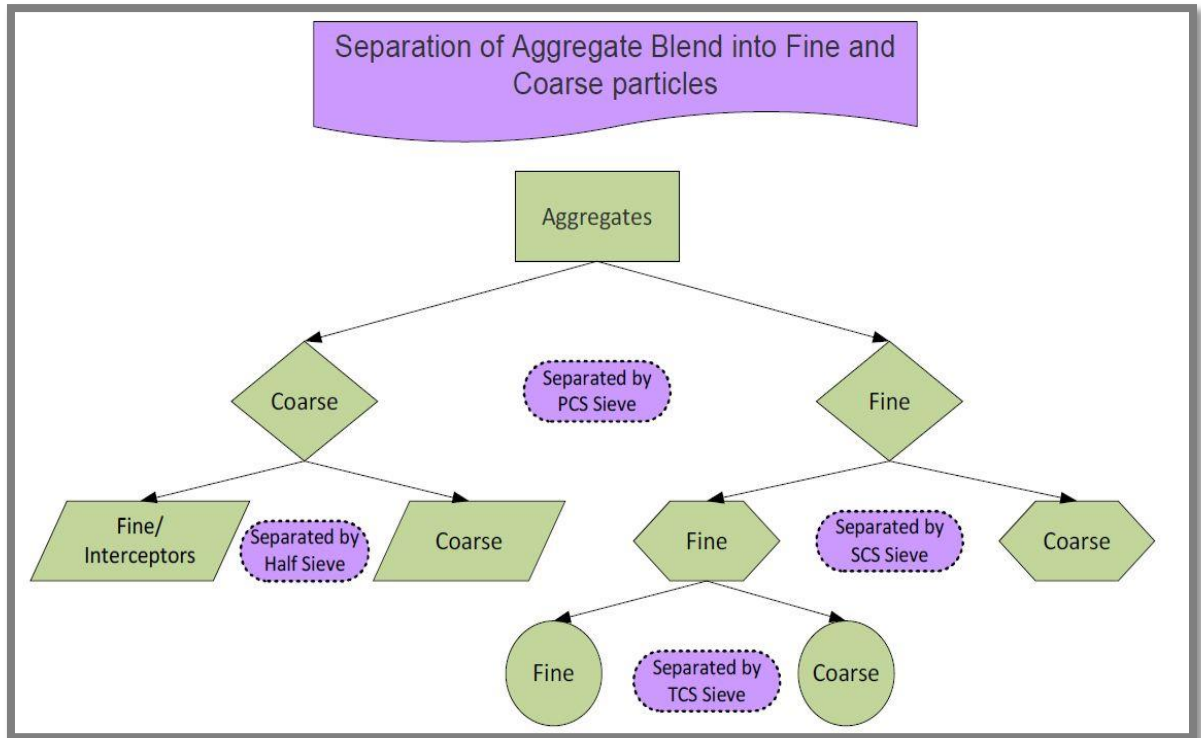


Figure 2 Flow Chart showing the separation of an aggregate blend into coarse and fine according to Bailey method

The SCS separates fine aggregates into fine and coarse, while the TCS separates the fine of the fines further into coarse and fine. On the other hand, the Half Sieve divides the coarse aggregate separated by the PCS into fine and coarse. The NMPS in this study is 12.5mm (1/2") and, therefore, the initial division between coarse aggregates and fine aggregates is sieve #8.

### 3.2.1.2 Chosen Unit Weight

In order to calculate the optimum gradation, the Bailey method requires the calculation of the unit weight. This value depends on determining the loose and rodded unit weight for the coarse aggregates and the rodded unit weight for fine aggregates. The values are obtained according to the shoveling and rodding procedure respectively outlined in AASHTO T19. The calculated loose unit weight (LUW) is the lower limit of coarse aggregate interlock. Theoretically, it is the dividing line between fine-graded and

coarse-graded mixtures. The rodded unit weight (RUW) is generally considered to be the upper limit of coarse aggregate interlock for dense-graded mixtures. This value is typically near 110% of the loose unit weight. **Table 1** shows the effect of the percent chosen of LUW used to the corresponding mix formed.

Table 1 Chosen UW as a percent of LUW and the corresponding mix performance

Chosen Unit Weight (CUW)	Corresponding mix formed
< 90% LUW	The coarse aggregates are spread apart
90-95% LUW	Dense graded mix/ Fine aggregate skeleton is developed
95-105%LUW	Dense graded mix/coarse aggregate interlock is developed
105% LUW	Coarse aggregate skeleton / Used when aggregates are soft and prone to degrade
> 105% LUW	Increased probability of degradation and difficulty in field compaction

The chosen unit weight is determined according to the gradation to be designed.

In this study the CUW was considered to be 103% LUW.

### 3.2.1.3 Ratios

The other parameters introduced by the Bailey method are the ratios that evaluate packing within the combined aggregate gradation:

- Coarse Aggregate Ratio (CA Ratio): describes how the coarse aggregate particles pack together
- Fine Aggregate Coarse Ratio (FA<sub>c</sub>): describe how the coarse portion of the fine aggregate packs together
- Fine Aggregate Fine Ratio (FA<sub>f</sub>): describes how the fine portion of the fine aggregate packs together

An aggregate gradation was determined using the Bailey method where for the given N.A stockpiles brought from the quarry the CA ratio was found out to be 0.76 which is higher than the required range presented in Table 2 below.

Table 2 Recommended Ranges of Aggregate Ratios

NMPS (mm)	37.5	25.0	19.0	12.5	9.5	4.75
CA Ratio	0.80-0.95	0.70-0.85	0.60-0.75	<b>0.50-0.65</b>	0.40-0.55	0.30-0.45
FAc Ratio	0.35-0.50	0.35-0.50	0.35-0.50	<b>0.35-0.50</b>	0.35-0.5	0.35-0.50
FAf Ratio	0.35-0.50	0.35-0.50	0.35-0.50	<b>0.35-0.50</b>	0.35-0.50	0.35-0.50

Moreover, it was observed that this gradation does not pass some of the Superpave limits. Since all aggregates are sieved into different sizes in the lab, minor adjustments were done to obtain a gradation that is within the acceptable ranges of Superpave design as shown in Figure 3.

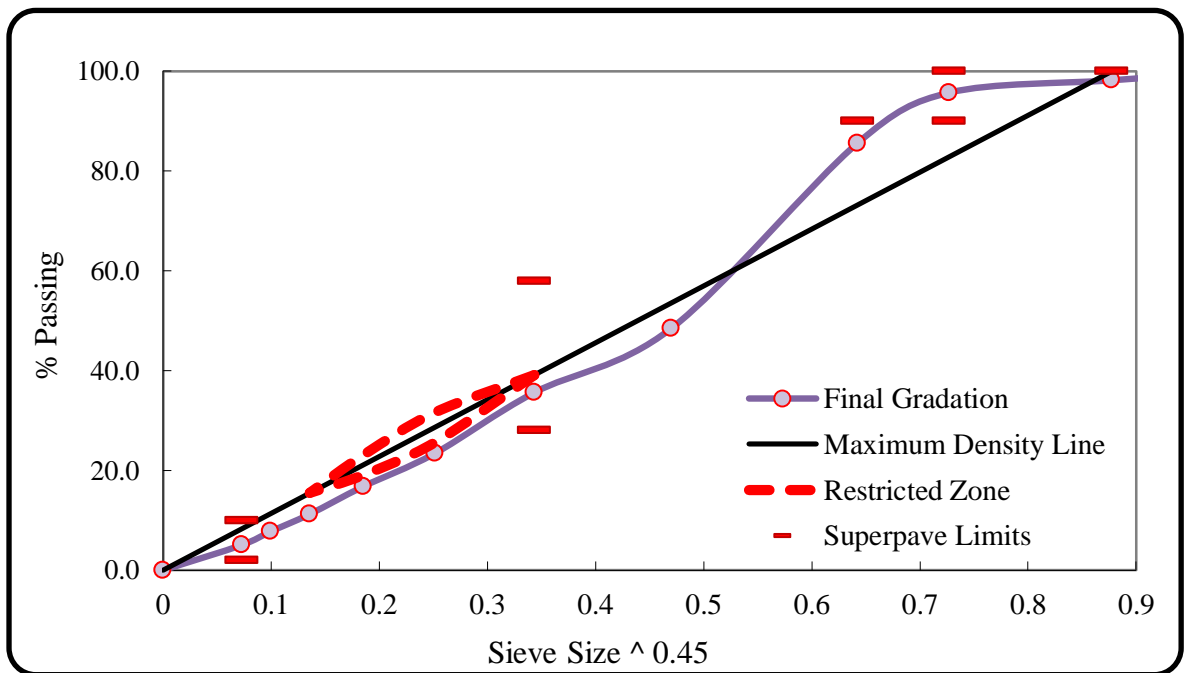


Figure 3 Aggregate gradation used in the mix design



At the same time, the adjusted aggregate gradation passed the three ranges of parameters according to Bailey method as shown in Table 3.

Table 3 Three calculated parameters and their corresponding ranges.

Parameters	Equation	Ratio	Range for NMPS=12.5mm
CA	$\frac{\% \text{ passing Half seive} - \% \text{ passing}}{100 \% - \% \text{ passing Half seive}}$	0.62	0.5-0.65
FA <sub>C</sub>	$\frac{\% \text{ passing SCS}}{\% \text{ passing PCS}}$	0.44	0.35-0.50
FA <sub>F</sub>	$\frac{\% \text{ passing TCS}}{\% \text{ passing SCS}}$	0.44	0.35-0.50

### 3.3 Marshall and Superpave Mix Design

Two main mix design methodologies are present for designing HMA; the Marshall Mix design and the Superpave Mix design. Marshall Mix design is limited when it comes to simulating real life compaction. Therefore, the goals of the new mix design (Superpave) for HMA pavements were to produce methods that would simulate the real stresses that a HMA pavement undergoes when being paved. The main limitation of Marshall Mix design method was the limited size of the sample that was 4", the first change that Superpave introduced was increasing the sample size to 6". In addition, the compaction mechanism was altered, where the mix is compacted at an angle of 1.25° with a vertical pressure of 600 kPa and a gyration rate of 30 revolutions per minute. This compaction method mimics the stresses in the field applied by the roller compactor on the pavement which are axial and shear stresses. In addition, Superpave introduced the larger specimen size for testing and the fabrication of the

specimens is done by coring and sawing a 4” specimen from the 6” specimen thus eliminating the effect of the boundary condition that typically includes higher air voids.

Although the Superpave is a newer methodology but several countries still use Marshall Method of design and compaction. Studies have shown that the Marshall hammer ranked the least in terms of ability to produce HMA mixtures having similar properties to field specimens (Von Quintus et al., 1989). Another study indicated that the gyratory method of compaction provides better results than any other compaction method (Button et al., 1994). Moreover, in a research studying the effect of compaction method on mixes having fractured coarse aggregates mixes compacted with the Superpave gyratory compactor had lower air voids than those compacted with Marshall hammer (Calberget al., 2003). In addition, the specimens compacted with Superpave showed a trend as the amount of fractured aggregates increased, however mixes compacted with Marshall did not show any trend indicating that the marshal hammer didn't mimic the real conditions (Calberg et al., 2003). Referring to Memon, the relationship between the Marshal number of blows and the number of Superpave gyrations is mix dependent (Memon, 2006). However, the optimum asphalt content according to Cho et al. (2010) determined by Superpave mix design method are not significantly different from those determined from the Marshall Mix design method for mixtures with natural coarse aggregates. Therefore, since Marshall and Superpave Mix design are the two most dominantly used design methods and since Lebanon still adopts the Marshall Mix design, the study will incorporate both Mix designs.

### ***3.3.1 Optimum Asphalt Content using Marshall Mix Design***

In order to determine the optimum asphalt content for a given aggregate gradation, 4 different asphalt contents (AC%) were considered as a percentage of the

total mass of each mix. The considered percentages were 3.5%, 4.0%, 4.5%, and 5.0%. After mixing, compacting, and testing the specimens, the optimum asphalt content is determined by the mix that provides 4% air voids.

For this study six different mixes were to be investigated. Since the aim of the study is to determine the effect of fine RCA on HMA, 6 replacement percentages were considered: 0%, 10%, 15%, 20%, 30%, and 45%. The replacement was done by weight therefore, for each fine sieve size (less than 4.75mm), the corresponding percentage of natural aggregates was replaced by fine RCA. For each of the 6 mixes, 3 specimens were compacted 75 blows corresponding to heavy traffic for testing of bulk specific gravity ( $G_{mb}$ ) according to ASTM 2726 and 2 specimens were left loose for testing for the theoretical maximum specific gravity ( $G_{mm}$ ) according to ASTM 2041. If a sample is an outlier another was prepared to verify value of either the  $G_{mm}$  or the  $G_{mb}$ . The weight of the compacted samples is 1200g determined from Asphalt Institute mix design handbook, while that of  $G_{mm}$  is determined based on the NMPS. ASTM 2041 specifies that for a NMPS of 12.5mm (1/2"), the minimum required weight is 1500g, thus for this study a weight of 1750g was considered for the loose mixes.

### ***3.3.2 Testing of Marshall Specimens***

#### ***3.3.2.1 Air Voids***

For each of the optimum asphalt contents, the samples were tested for  $G_{mb}$  and  $G_{mm}$  in order to determine the air voids of each sample using equations 2, 3 and 4. After determining the air voids of each mix at the four asphalt content, the optimum AC% is determined at 4% air voids.

$$G_{mb} = \frac{A}{(B-C)} \quad (2)$$

Where

*A*=mass of the dry specimen in air (g)

*B*= mass of the saturated surface-dry specimen in air (g)

*C*= mass of the specimen in water (g)

$$Gmm = K * \frac{A}{A+D-E} \quad (3)$$

Where

*A*= mass of dry sample in air (g)

*D*= mass of flask filled with water and cover plate at 25°C (g)

*E*=mass of flask filled with sample, cover plate, and water (g)

*K*= correction factor for water temperature

$$AV\% = 100 \left( 1 - \frac{Gmb}{Gmm} \right) \quad (4)$$

### 3.3.2.2 Voids in the Mineral Aggregates (VMA)

The VMA is defined as the void space that is between the aggregates of a compacted sample. This volume includes the air voids and the effective asphalt that is not absorbed by the aggregates.

$$VMA = 100 - \frac{Gmb * Ps}{Gsb} \quad (5)$$

Where

*Ps*: percent of aggregate content in the mix (%)

*Gsb*: Bulk specific gravity of total aggregate

*Gmb*= Bulk specific gravity of compacted mixture

### 3.3.2.3 Voids filled with Asphalt (VFA)

The VFA is defined as the percent of volume of VMA that is filled with asphalt cement (the effective asphalt binder)

$$VFA = 100 * \frac{VMA - Va}{VMA} \quad (6)$$

### 3.3.2.4 Stability and Flow

The Marshall stability is defined as the maximum load required to cause failure when a specimen is tested under a constant loading rate of 51mm/minute. When the load starts to decrease the maximum load is recorded. Simultaneously, the vertical deformation is determined using a dial gauge at the maximum load. This is the recorded as the flow and is expressed in units of 0.25mm. From the stability reading, the uncorrected stability is calculated using equation 7 below which is dependent on the type of dial reader used

$$\text{Uncorrected Stability}(lbs) = -0.2392 * (\text{dial reading})^2 + 105.58 * (\text{stability reading}) - 9.7363 \quad (7)$$

After calculating the uncorrected stability and depending on the thickness of the sample, the stability is calculated using equation 8.

$$\text{Corrected Stability}(Kgs) = 0.45359237 * \text{Uncorrected Stability}(lbs) * K \quad (8)$$

where

*K*: stability correlation ratio calculated based on the thickness of the sample obtained from the ASTM standard

0.45359237: conversion factor from lbs to Kgs

The flow is calculated using equation 9

$$flow(0.25mm) = \frac{0.01 * flow(0.01mm)}{0.25} \quad (9)$$

In order to evaluate the calculated volumetrics, stability, and flow, Marshall Method specifies mix design requirements presented in Table 4 and Table 5; the highlighted cells are those applicable to the mix design adopted in this study.

Table 4 Marshal Design criteria

Compaction , number of blows each end of specimen	35		50		75	
Design ESAL	< 10 <sup>4</sup>		Between 10 <sup>4</sup> and 10 <sup>6</sup>		>10 <sup>6</sup>	
Stability (Kgs)	340		545		818	
Flow, 0.25mm	8	18	8	16	8	14
Percent Air Voids	3	5	3	5	3	5
Percent Voids Filled with Asphalt (VFA)	70	80	65	78	65	75

Table 5 Minimum percent voids in mineral aggregates

Nominal Maximum Particle Size		Design Air Voids, Percent		
		3.0	4.0	5.0
mm	in.			
1.18	No.16	21.5	22.5	23.5
2.36	No.8	19.0	20.0	21.0
4.75	No.4	16.0	17.0	18.0
9.5	3/8	14.0	15.0	16.0
12.5	½	13.0	14.0	15.0
19	¾	12.0	13.0	14.0
25	1.0	11.0	12.0	13.0
37.5	1.5	10.0	11.0	12.0
50	2.0	9.5	10.5	11.5
63	2.5	9.0	10.0	11.0

### 3.3.2.5 Moisture Sensitivity

Shifting into Superpave with no clear test for moisture sensitivity testing, several agencies are adopting the AASHTO T283 as the test procedure. A study conducted by Ohio department of Transportation indicated that the Gyrotory compacted specimens sized 150mm in diameter could be used to determine the TSR (Liang, 2008). Another study by McCann et al. (2001) used the ultrasonic moisture accelerated conditioning process to quantify the moisture sensitivity of HMA mixes. The study concluded that in order to generate similar conditioning of the ultrasonic moisture 18 freeze-thaw cycled are needed. Another study by Choubane et al. (2000) recommended that the test samples be saturated to more than 90%, the freeze-thaw cycled should not be optional, and the air voids range should be narrowed to 6.5%-7.5%.

In order to study the moisture sensitivity of the RCA mixes, specimens will be prepared using the optimum % AC determined from Marshal Mix Design for 3 RCA percentage replacements: 0%, 15%, and 30%.

The specimens will be divided into two subsets having the same target air voids; one to be maintained dry while the other partially saturated with water and moisture conditioned. AASHTO T 283 requires that specimens be compacted to  $7\pm 1\%$  air voids for this the number of blows was reduced in order to obtain the desired air voids. After that the average tensile strength of the dry subset and that of the moisture conditioned subset are determined, and the Tensile Strength Ratio (TSR) is calculated.

### ***3.3.3 Testing of Superpave Specimens***

Having determined the optimal asphalt content using Marshal Mix design, the obtained mixes will be considered for Superpave specimens. For each mix, three

replicate Superpave specimens will be prepared. The specimens will be tested to determine if the optimum mix determined for the marshal mix is the same optimal mix at  $N_{des}$ . To determine this, the 4% air void will be the evaluating criteria to determine if the mix is optimal. In addition, the mixes will be evaluated to make sure they pass Superpave criteria: required density at  $N_{ini}$ ,  $N_{des}$ ,  $N_{max}$ , Voids in mineral aggregates (VMA), and Voids filled with asphalt (VFA). Since the Marshall mixes were designed for heavy traffic which corresponds to a design Equivalent Single Axial Load (ESAL) greater than  $10^6$ , the Superpave samples were compacted to the equivalent number of gyrations for medium to high traffic. The Values of  $N_{ini}$ ,  $N_{des}$ , and  $N_{max}$  were 8, 100, and 160 gyrations respectively. Table 6 below indicates the Superpave requirements; the highlighted cells are those applicable to the mix design adopted in this study.

Table 6 Superpave design requirements

Design ESALs (million)	Required Density (% of theoretical maximum specific gravity)			Voids in the Mineral Aggregate (Percent), minimum					Voids filled with asphalt (Percent)
	Ninitial	Ndesign	Nmax	Nominal Maximum Aggregate Size, mm					
				37.5	25	19	12.5	9.5	
< 0.3	< 91.5								70-80
0.3 to < 3	≤ 90.5								65-78
3 to <10	≤ 89.0	96	≤ 98.0	11.0	12.0	13.0	14.0	15.0	65-75
10 to < 30									
≥ 30									

### 3.3.3.1 Volumetric Testing

Similar to the Marshall Mix design testing, the air voids for the Superpave samples were determined and using equations 2, 3, and 4 above. Furthermore, the



percent of water absorbed is calculated for each sample to ensure that it is less than 2%. This is done to ensure that there is no need to change the method of calculating the  $G_{mb}$  and use parafilm. In addition, the VMA and VFA were calculated. Moreover, the required density at  $N_{ini}$  is calculated to check that the mix passes the criteria. 2 samples will then be compacted to  $N_{max}$  to ensure that the required density is satisfied.

### 3.3.3.2 Dynamic Modulus Testing

The complex modulus ( $E^*$ ) is used to represent the stress strain relationship of linear viscoelastic materials under a continuous sinusoidal load. Being a viscoelastic material, the dynamic modulus is affected by the HMA mix properties, frequency of testing, the test temperature, and the specimen geometry (Tashman and Elangovan, 2007). The complex modulus test entails applying a uniaxial sinusoidal compressive stress to an unconfined HMA sample and determining the strains in order to compute the dynamic modulus (the absolute value of the complex modulus  $|E^*|$ ). Being a complex number, the complex modulus has both real and imaginary parts, the storage and loss moduli respectively as shown in below in equation 10.

$$E^* = E' + iE'' \quad (10)$$

Where

$E'$  = Storage Modulus,

$E''$  = Loss Modulus, and

$i = \sqrt{-1}$ .

Therefore, the magnitude of the complex modulus (dynamic modulus) is defined as shown in equation 11.

$$|E^*| = \sqrt{E'^2 + E''^2} \quad (11)$$

The storage and loss moduli are related to the dynamic modulus as shown in equations 12 and 13. The more the material is elastic the more the phase angle ( $\phi$ ) tends to decrease, a pure elastic material has  $\phi = 0^\circ$ . Similarly, the more the material is viscous the more the phase angle tends to increase, a pure viscous material has  $\phi=90^\circ$ .

$$E' = |E^*| \cos \phi \quad (12)$$

$$E'' = |E^*| \sin \phi \quad (13)$$

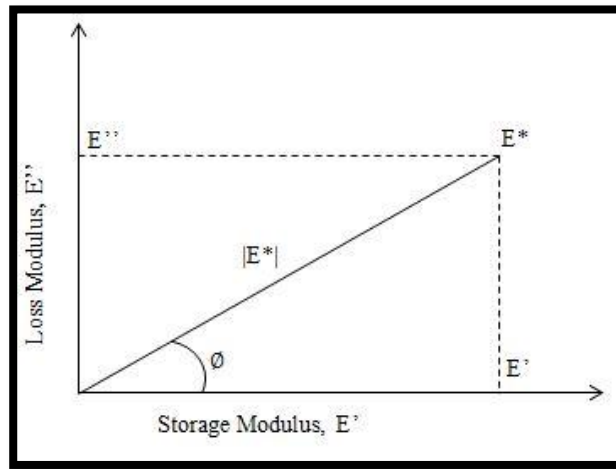


Figure 4 Complex modulus graphical representation (After Chehab. 2002)

The dynamic modulus and phase angle are usually tested at different temperatures and different loading frequencies in order to characterize the HMA material behavior in the field. Considering the wide range of temperature change between different regions, and the different vehicular speeds that can be encountered, the testing temperatures need to vary from low temperatures to represent cold climates and high temperatures to represent hot climates, and varied loading rates to represent fast and slow vehicular speeds. However, conducting the test for each temperature and for all loading rates would be rigorous along with the fact that there is a machine limitation to that. Therefore, applying the time-temperature superposition principle will help in providing the material response under predetermined temperatures and

frequencies that can then be shifted to construct the dynamic modulus master curve at a reference temperature. This principle entails that a certain dynamic modulus value at a reference temperature can be measured either at a higher temperature and lower frequency, or at a lower temperature and higher frequency. These measured values can be then shifted by the shift factor  $a_T$  that is multiplied by the testing frequency to obtain the reduced frequency at the reference temperature and thus construct the dynamic modulus master curve. These shifted data can then be fitted into a sigmoidal fit shown in equation 15.

$$a_T = \frac{fr}{f} \quad (14)$$

where

$a_T$ : shift factor at a given temperature

$fr$ : reduced frequency at the reference temperature

$f$ : frequency at a given temperature

$$\log(E^*) = a + \frac{b}{c + \frac{f}{\exp^{d+e \cdot \log(fr)}}} \quad (15)$$

where

$E^*$ : dynamic modulus (MPa)

$a, b, c, d, e,$  and  $f$ : fitting parameters

$fr$ : Reduced frequency, Hz

NCHRP report 465 defines a simple performance test as “A test that accurately and reliably measures the mixture response characteristics or parameter that is highly correlated to the occurrence of pavement distress over a diverse range of traffic and climatic conditions” (Witczak et al., 2002). The report recommended tests to determine material properties to address three distresses: rutting phenomenon through the dynamic

modulus and phase angle, the flow time and flow number, fatigue cracking through dynamic modulus, and thermal cracking through the creep compliance (Witczak et al., 2002). NCHRP Project 1-37A further indicated that the dynamic modulus is the main property needed for HMA pavement structural design (Tashman and Elangovan, 2007). For this, the dynamic modulus test was conducted on each of the mixes; two specimens were prepared for testing according to AASHTO T 342. The specimens were compacted to a height of 175mm and then cored and sawed to a height of 150 mm with a diameter of 101.6mm. The compaction direction was marked to record the orientation of the specimens during compaction, and the specimens were stored and tested in the same orientation as they were compacted. The target air voids was  $4\pm 0.5\%$ ; the weight required to obtain the target air void was obtained by trial and error. The machine used is a UTM-25 having a 25kN capacity. The machine has the capability to apply frequencies between 0.01 to 25Hz and temperatures between  $-10^{\circ}\text{C}$  and  $60^{\circ}\text{C}$ . The test was conducted on 4 temperatures:  $-7^{\circ}\text{C}$ ,  $10^{\circ}\text{C}$ ,  $25^{\circ}\text{C}$ , and  $40^{\circ}\text{C}$  at frequencies of 0.01Hz, 0.1Hz, 1Hz, 5Hz, 10Hz, and 20Hz in order to construct the dynamic modulus master curve. Some samples were tested at  $0^{\circ}\text{C}$  to ensure the overlap between the data from  $-7^{\circ}\text{C}$  and  $10^{\circ}\text{C}$ . The axial deformations were measured using 3 spring loaded linear variable differential transducers (LVDTs) that were mounted at 120 degrees apart along the circumference of the sample with a gage length of 100 mm. Testing was done from the lowest temperature to the highest and within each temperature from the highest frequency to the lowest. In order to ensure that the sample is undamaged during testing, the loading at each temperature and frequency was previously determined in order to provide a strain of 60-70 micro-strains a range that provides linear viscoelastic response, the micro-strains should not exceed 100 to ensure that the sample was not subjected to damage (Chehab, 2002). For this, a sample was prepared in order to

determine the load combination for each frequency and temperature. The starting loads were determined from a study previously conducted on Lebanese mixes at the American University of Beirut and then these loads were adjusted to obtain a value close to 75 micro-strains. The different load combinations used are represented in Table 7 below.

Table 7 Loads used in the dynamic modulus test for each temperature frequency combination

Frequency (Hz)	No. of Cycles	Stress (KPa)				
		Temperature (°C)				
		-7	0	10	25	40
Preconditioning 20	100	1000	850	700	370	80
20	200	2400	1915	1430	670	120
10	200	2380	1865	1350	530	96
5	100	2350	1800	1250	430	70
1	20	2210	1613	1015	250	35
0.5	15	2130	1523	915	190	28
0.1	15	1980	1335	690	90	16
0.01	10	1790	1085	380	38	-
Seating load		80	65	50	20	15
Rest Period between sweeps		5	5	5	5	10

A sample of the same material was prepared in order to monitor the temperature of the sample to be tested; a thermocouple was embedded inside and used as the control temperature reading. The sample was conditioned similarly to the sample to be tested. During the test, the raw data of the applied load and the measured axial deformation of each of the 3 LVDTs was recorded through an Integrated Multi Axis Control System (IMACS) at a rate of 50 points per cycle. This data was then analyzed by considering

the last 5 cycles of each temperature frequency combination. The stress and strain data was fitted to cosine functions shown in equations 16 and 17 using the least square method. The dynamic modulus is defined as the average peak stress divided by the average peak strain as shown in equation 18 while the phase angle is the difference between the phase angle of the stress and the strain.

$$\sigma = \sigma_0 \cos(2\pi ft + \phi_1) + \sigma_1 \quad (16)$$

$$\varepsilon = \varepsilon_0 \cos(2\pi ft + \phi_2) + \varepsilon_1 t + \varepsilon_2 \quad (17)$$

where

$\sigma$ : stress

$\varepsilon$ : strain

$t$ : time in sec

$f$ : frequency in Hz

$\sigma_0$ ,  $\sigma_1$ , and  $\phi_1$  = regression constants for stress equation

$\varepsilon_0$ ,  $\varepsilon_1$ ,  $\varepsilon_2$ , and  $\phi_2$  = regression constants for strain equation

$$|E^*| = \frac{\sigma_0}{\varepsilon_0} \quad (18)$$

$$\phi = \phi_2 - \phi_1 \quad (19)$$

where

$|E^*|$ : dynamic modulus

$\phi$ : phase angle

### 3.4 Mastic Testing

In order to better understand the behavior of the mix, the rheological properties of the mastic (binder+ filler) will be studied. The Dynamic Shear Rheometer (DSR) is used to determine the Complex Shear Modulus ( $G^*$ ) at intermediate and high service temperatures for asphalt binders according to ASTM 7175-08. For low temperatures the

Bending Beam Rheometer (BBR) data is need in order to develop the master curve of  $G^*$  which will not be included in this study. Replicates of two will be used to determine the high temperature performance grade of the samples presented in Table 8. The sample used has a diameter of 25mm and a thickness of 1mm. The test is strain controlled where an oscillatory strain of 12% is applied. The  $G^*$  and phase angle are considered at an angular frequency of 10rad/sec. All mastics were produced at a 1:1 mixing ratio of filler to binder by mass in accordance with the Superpave specification, which recommends the mass ratio of filler to bitumen be in the range of 0.8 to 1.2 and according to Bahia's recommendation where blending on a 1:1 ratio corresponds to the typical filler concentration in HMA (Fahem and Bahia, 2010).

Table 8 Sample to be tested for the mastic study

Sample Type	Percentage of Natural Filler	Percentage of Recycled Filler
B	0%	0%
B-1N	100%	0%
B-0.85N-0.15R	85%	15%
B-0.7N-0.3R	70%	30%
B-1R	0%	100%
B-1H	0%	100%

B: binder , xN: ratio of natural filler, yR: ratio of recycled filler,

zH: ratio of hydrated cement

In addition to determining the complex modulus of the above samples, the viscosity will be determined starting with a temperature of 125°C and increasing to a temperature of 150°C with an increment of 5°C. The sample is placed in a concentric

cylinder where an increasing shear rate is applied. The viscosity is calculated by averaging the reading around  $10\text{sec}^{-1}$ . A typical sample volume required is 23ml. In addition, the multiple stress creep and recovery test will be conducted on the samples. This test method covers the determination of percent recovery and non-recoverable creep compliance of asphalt binders/mastics. Non recoverable creep compliance is an indicator of the resistance to permanent deformation under repeated load. The sample used is a 25mm specimen that is subjected to 20 creep and recovery cycles the constant stress is applied for 1 second and then allowed to recover for 9 seconds. During the first 10 cycles the stress applied is 0.1 kPa, while during the remaining 10 the stress applied is 3.2 kPa.



## CHAPTER 4

### RESULTS AND ANALYSIS

#### 4.1 Material Properties

##### 4.1.1 Aggregates

The calculated values of specific gravity reveal the difference between the fine natural aggregates (NA) and the fine recycled concrete aggregates (RCA). The fine RCA exhibits a lower specific gravity which indicates that for an equivalent mass, the fine RCA will occupy a slightly higher volumetric proportion in a HMA mixture. In addition, the absorption of the fine RCA is higher than that of the fine NA; this suggests that to maintain the same asphalt film thickness, higher asphalt content would be needed when using fine RCA. Moreover, the sand equivalent test reveals a lower value for fine RCA indicating the presence of more dust and fine particulates when compared to the fine NA. The results of these properties are presented in Table 9. The results just stated can be revealed in the microscopic images of both the fine NA and fine RCA. As shown in figures 5 and 6, the SEM images clearly show that the surface of the NA is smooth while that of RCA is much rougher and includes more pores thus leading to higher absorption. In addition, the SEM images shown in Figure 7, 8 and 9 for the filler material show the presence of more dust particles thus revealing the lower value of sand equivalence. Two samples of the natural and recycled filler were tested to calculate the surface area. The results in Table 10 reveal that the recycled filler has a higher surface area than the natural filler by a ratio of 3.1:1. In addition, the compressive strength of the recycled aggregates and the natural aggregates was measured and shown in Table 11 which showed a higher strength for natural limestone aggregates.

Table 9 Specific gravity and absorption of RCA and natural aggregates

Property	Coarse NA	Fine NA	Fine RCA
Specific gravity	2.750	2.668	2.236
Absorption capacity	0.55%	0.20%	5.29%
Sand equivalent	----	48%	39%

Table 10 Surface area of recycled and natural filler

Replicate	Surface Area (m <sup>2</sup> /g)	
	Natural	Recycled
1	2.85	8.01
2	2.68	8.94
Average	2.76	8.47

Table 11 Compressive strength of recycled and natural aggregates

Type of Aggregate	Compressive Strength (MPa)
Recycled concrete	34
Natural limestone	75

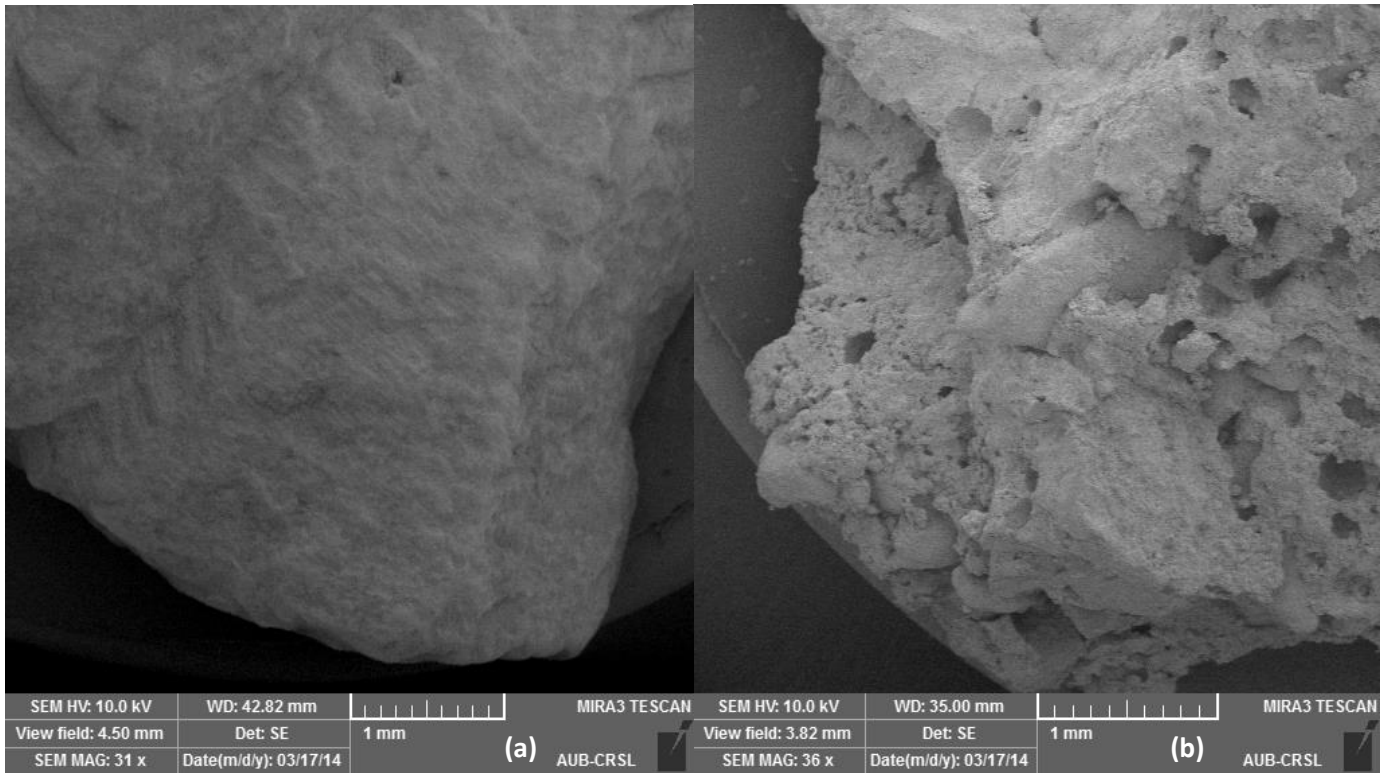


Figure 5 SEM images of (a) natural aggregates and (b) recycled aggregates

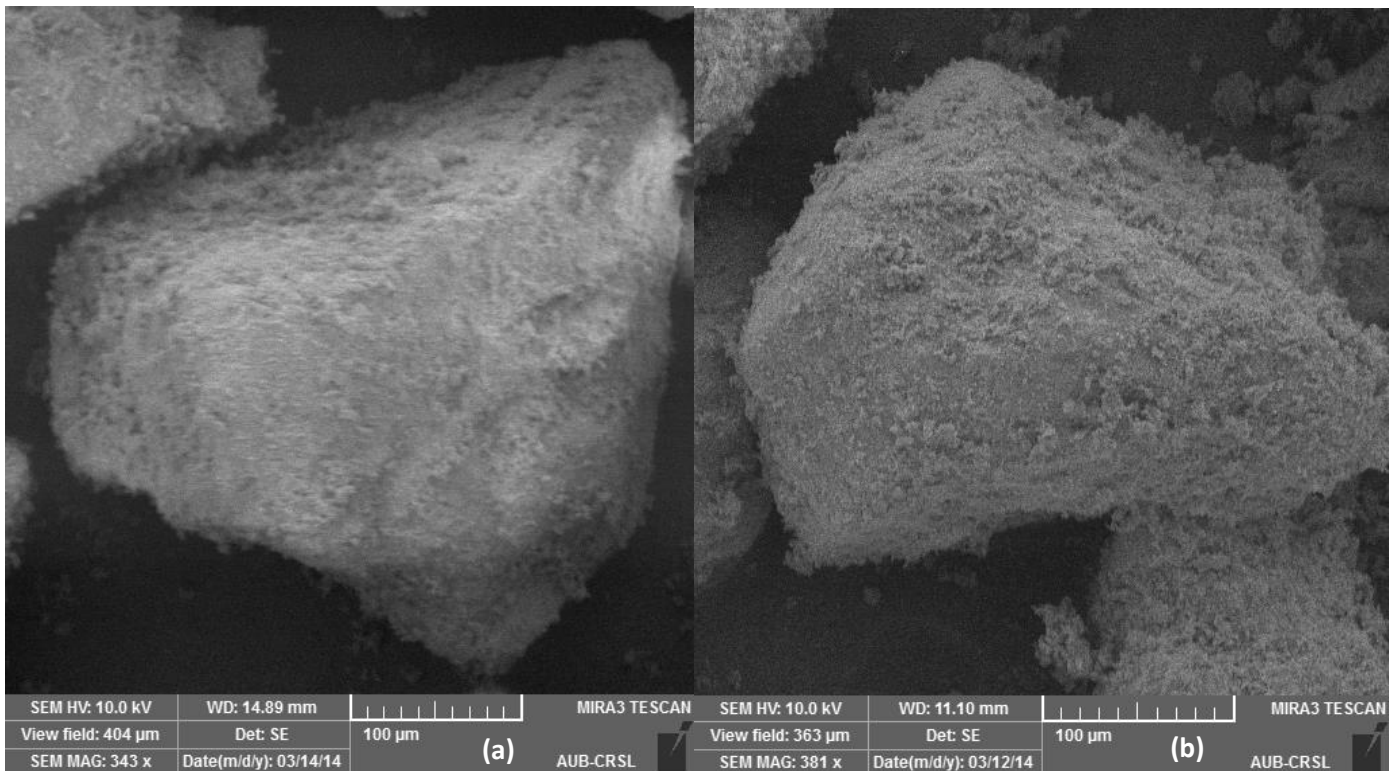


Figure 6 SEM images of #100(0.15mm) size (a) natural aggregate and (b) recycled aggregates

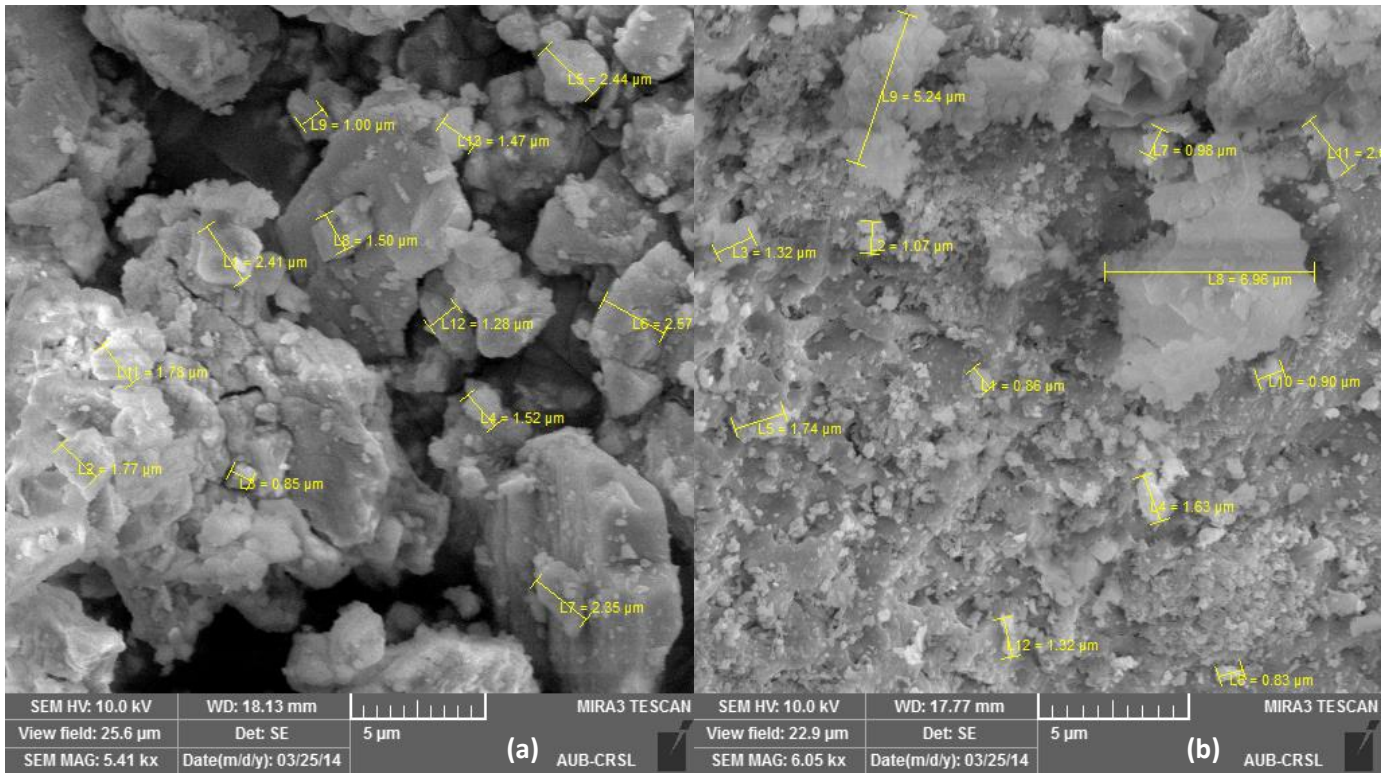


Figure 7 SEM images of passing #200(00.75mm) size (a) natural aggregate and (b) recycled aggregates

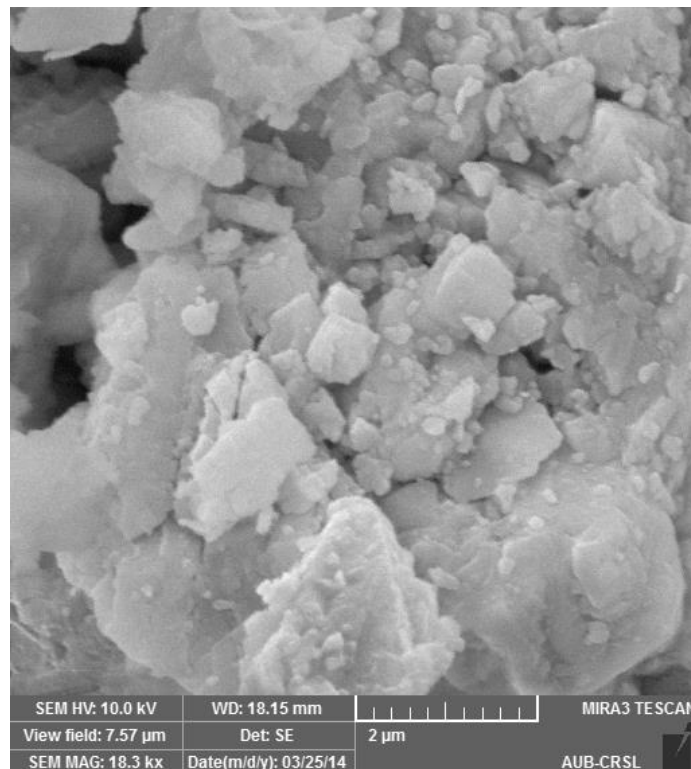


Figure 8 SEM image of natural pan at 2 um

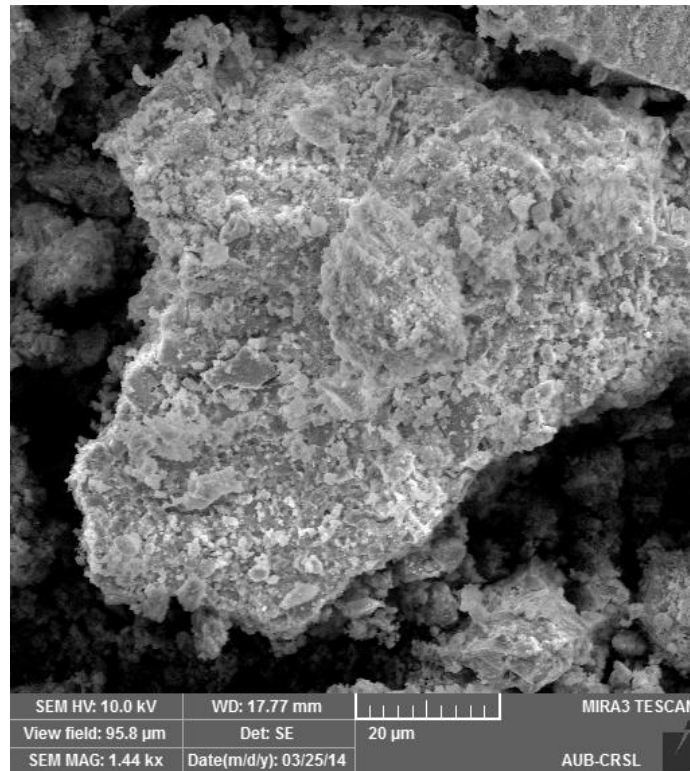


Figure 9 SEM image of Recycled pan at 20um

#### 4.1.2 Asphalt Binder

The penetration test performed on the binder indicated that it is a Pen60-70 binder as indicated by the supplier, the ductility measure was 120 cm and the softening point was 54°C. The binder was tested at 6 grading temperatures and the value of  $\frac{G^*}{\sin(\gamma)}$  was calculated at 10rad/sec, the PG grade obtained was 64°C which is consistent with the results of Marshal binder testing. The results are shown in Figure 10 .

Table 12 Results of tests performed on asphalt binder

Test	Result
Ductility	120 cm
Penetration	60-70
Softening	54 (degree Celsius)

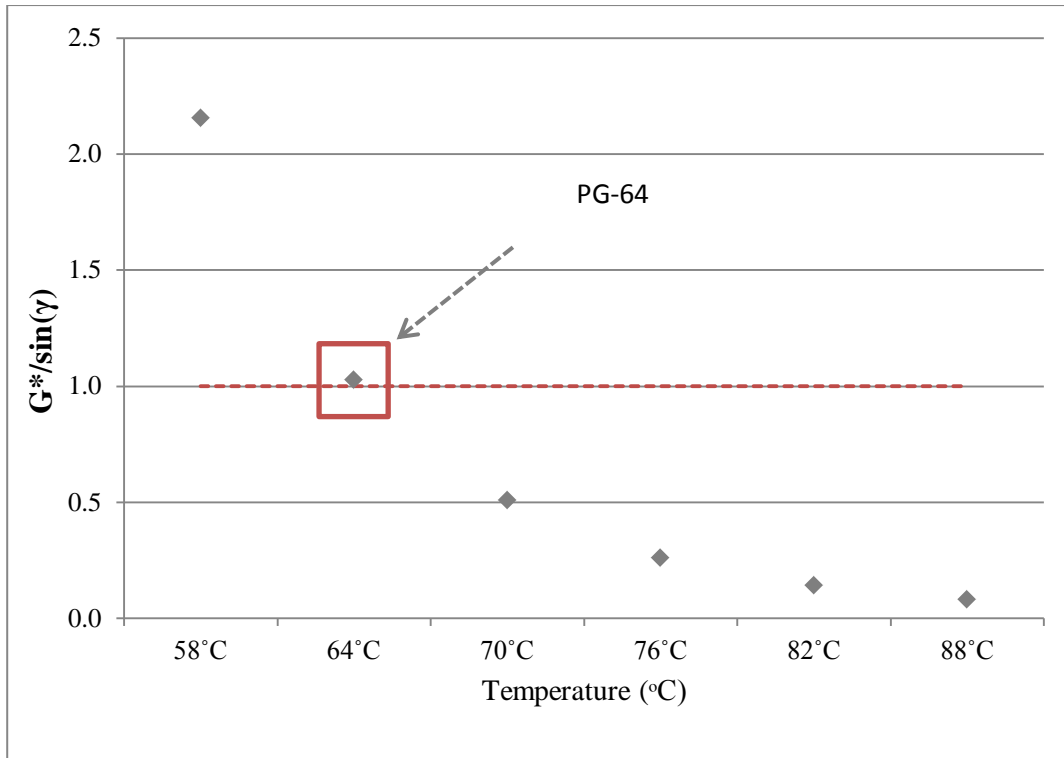


Figure 10 Binder  $G^*/\sin(\gamma)$  values for different tested temperatures

#### 4.2 Marshal Mix Design

As mentioned earlier, 6 replacement percentages of fine natural aggregates were considered; 0%, 10%, 15%, 20%, 30%, and 45%. For such percentage replacement of fines, the RCA constituted 0%, 4.9%, 7.3%, 9.7% , 14.6% and 21.8% of the total aggregate weight respectively. For these mixes, 4 AC% were considered in order to obtain the optimum asphalt content. Figure 11 shows the AV% as a function of AC% for each of the considered mixes. For the 45% RCA mix an additional AC% was required in order to achieve the optimum AC%

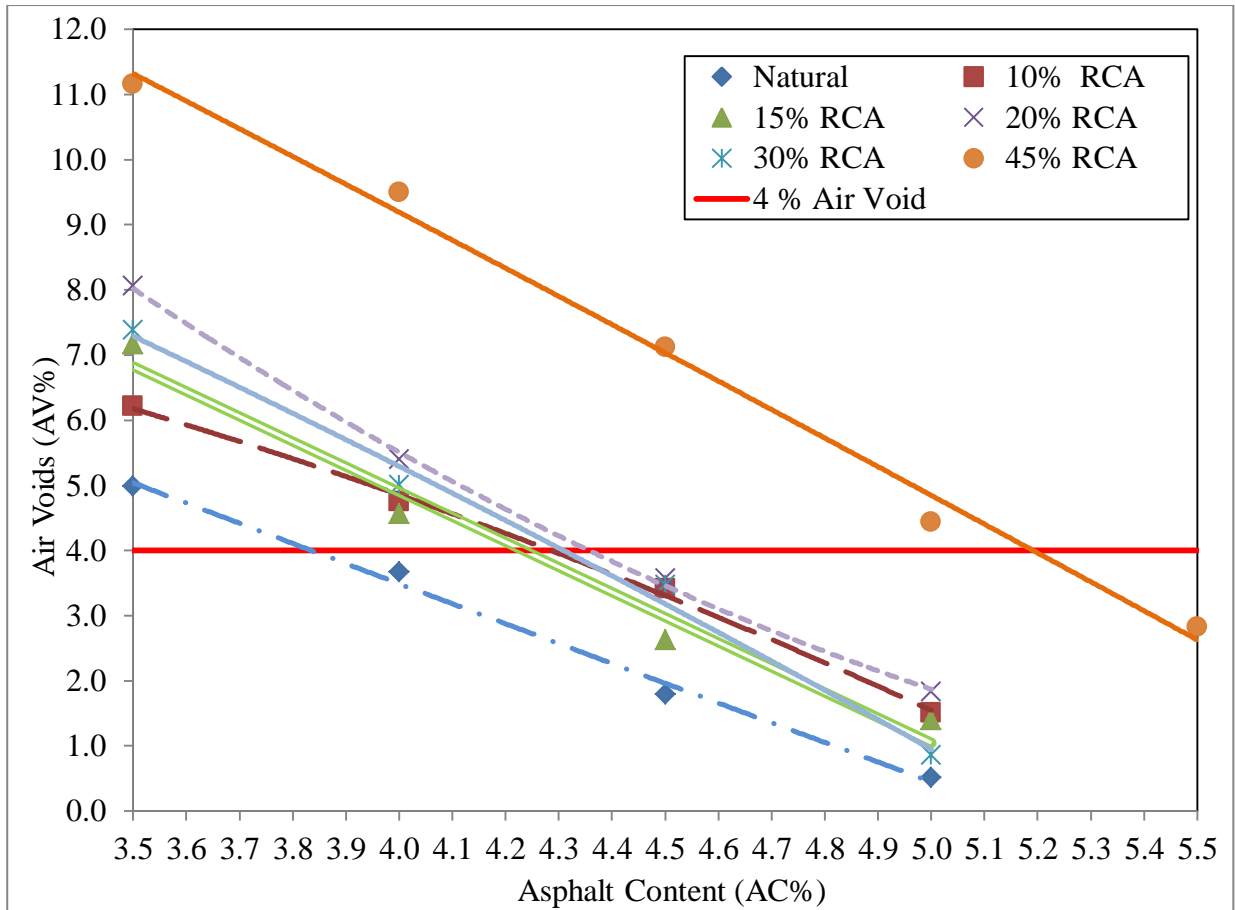


Figure 11 AV% versus AC% for the six mixes

The results in Figure 11 reveal that for each of the AC% in the study, mixes with RCA have a higher AV% than those for control (natural aggregates only). This trend increases significantly when the replacement reaches 45%; an increase of 1.4% from the optimum AC% of the natural mix is noted. This upward shift increases the AV% by 5% for each AC%. In order to ensure a beneficial outcome from the replacement of natural aggregates with fine RCA, a need to maximize the use of RCA percentage and maintain the AC% in an acceptable increase. The use of 45% RCA fails to be justifiable due to the high increase in AC% and therefore will not be considered for the rest of the study. Looking at the trends for the remaining replacement percentages, an interchange of the curves is present. No clear trend of AC% increase as RCA% increase is evident;

however the curves indicate close asphalt content of 4.3% between the 10%, 15%, 20%, and 30% RCA curves as shown in Table 13 below.

Table 13 Optimum asphalt content for each of the 6 mixes

RCA % in mix	AC%
0	3.84
10	4.29
15	4.24
20	4.36
30	4.31
45	5.19

Based on the obtained asphalt contents of the mixes, moving from a mix with natural aggregates to a mix with fine RCA a mere additional value of 0.4% asphalt content is needed. Based on the %RCA needed to be added a slight addition of 0.15% is needed to move from 10% RCA to 30% RCA. Thus the use of 30% is recommended because it provides a slight increase in AC% between the other percent RCA replacement.



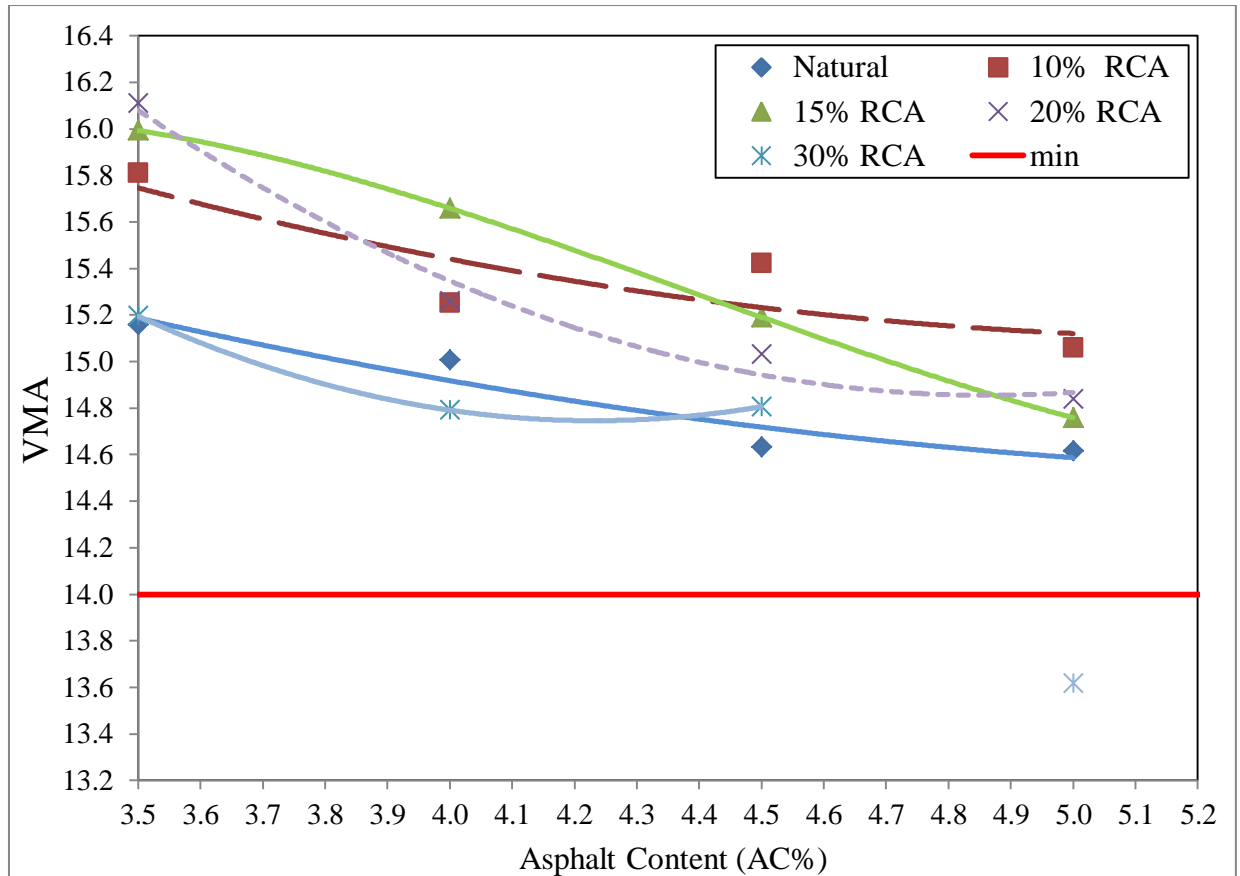


Figure 12 VMA versus AC% for the six mixes

Observing the VMA values for the natural mix, as the AC% increases the VMA decreases. This is because as the AC% increases the mix becomes more workable and compacts more easily. Hence up to 4.5% AC, the same weight can be compacted into a less volume. After this AC%, the effective binder increases in the mix were no further compaction can occur thus the effective binder increases taking the place of the AVs. This increase in AC% and decrease in AV% had an equal and opposite effects that lead to no change in the VMA value. In order to better understand the change in VMA, Table 14 below shows the volume of the effective binder ( $V_{\text{beff}}$ ) that is the AV% subtracted from the VMA. Comparing the VMA values of the mixes at 3.5%, the  $V_{\text{beff}}$  decreases as the %RCA increases in the mix this is due to the effect of the RCA that is absorbing the asphalt and thus decreasing the asphalt remaining in the mix.

Table 14 Volume of effective binder for each asphalt content for each of the five mixes

	%RCA				
AC%	0%	10%	15%	20%	30%
3.5%	10.18	9.60	8.82	8.05	7.81
4.0%	11.34	10.50	11.09	9.80	9.79
4.5%	12.84	12.01	12.58	11.46	11.34
5.0%	14.11	13.55	13.36	13.06	12.79

Comparing the 10 and 15 % to the natural mix, the same trend can be observed, the higher values are attributed to the AV% since the mixes have a higher volume due to the new introduced material. The drop in VMA at 5% asphalt content for the 15% RCA mix is attributed to the lower  $V_{\text{beff}}$ . At this amount of AC%, the mix becomes very workable and more compactable thus less AV%; the decrease in AV% and decrease in  $V_{\text{beff}}$  leads to a drastic decrease in VMA. Similarly to the 20% RCA, however, the drop in VMA starts at a lower AC% than that of 15%, this decrease is due to the  $V_{\text{beff}}$  that is less in the mix due to the higher absorptive property that is in the mix. In the 30% mix, the drop in VMA starts at low AC%, the RCA aggregates in the mix have a huge effect. Although the AV% are similar to the remaining RCA mixes, however the  $V_{\text{beff}}$  is a lot less due to the higher absorption of the material that caused the VMA to drop. At 5% asphalt content, the mix has sufficient binder that allows it to be compacted easily, the RCA absorbed the needed binder and with the remaining the mix is more compactable and thus less air voids and less VMA.

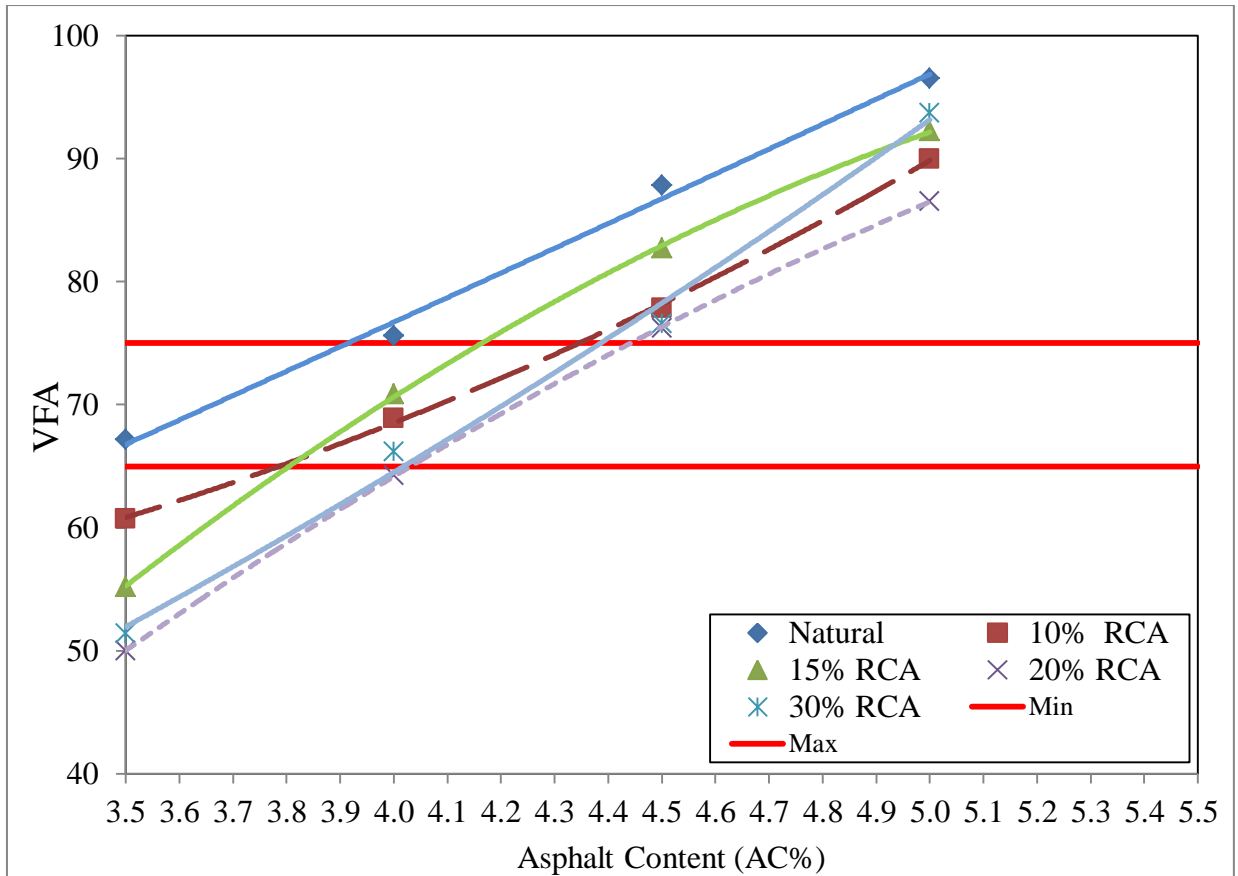


Figure 13 VFA versus AC% for the six mixes

The VFA is consistently higher for the natural mix as shown in Figure 13. This can be attributed to the higher air voids in the RCA mixes thus leading to less volume for the effective binder and hence a lower VFA values for the RCA mixes

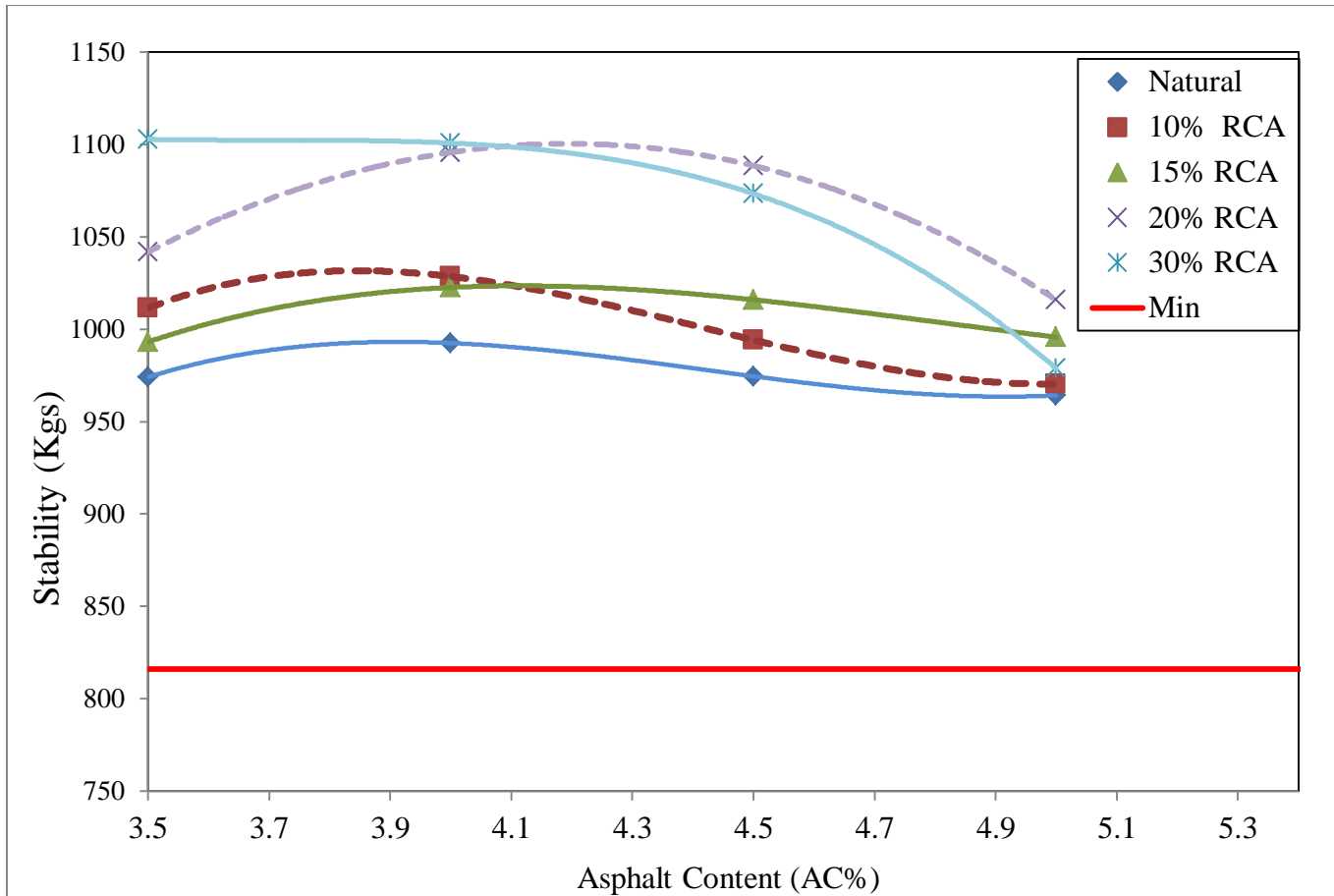


Figure 14 Stability versus AC% for the five mixes

All RCA mixes have a higher stability than the control mix at all asphalt contents. Knowing that the coarse aggregates in these mixes are the same, the higher strength can be attributed either to the mastic or the fine aggregate matrix. Comparing the 10%, 15%, and 20% RCA, close to the optimum asphalt content (4.3%), as the amount of fine RCA increases the stability of the mix increases. However, as the % RCA increases to 30% the stability decreases but still remains greater than the natural mix. This indicates that the addition of RCA up to 30% increases the strength of the HMA causing it to withstand higher loads before failing. Up to 20% RCA, even at high asphalt contents the mix provided a better performance than the natural mix indicating that 20% might be the limiting percentage when using fine RCA.

Looking at the flow results for the mixes, the actual values can't be interpreted.

The results don't represent the material behavior. This can be attributed to the dial gauge and setup that is used. The results are presented in Figure 15.

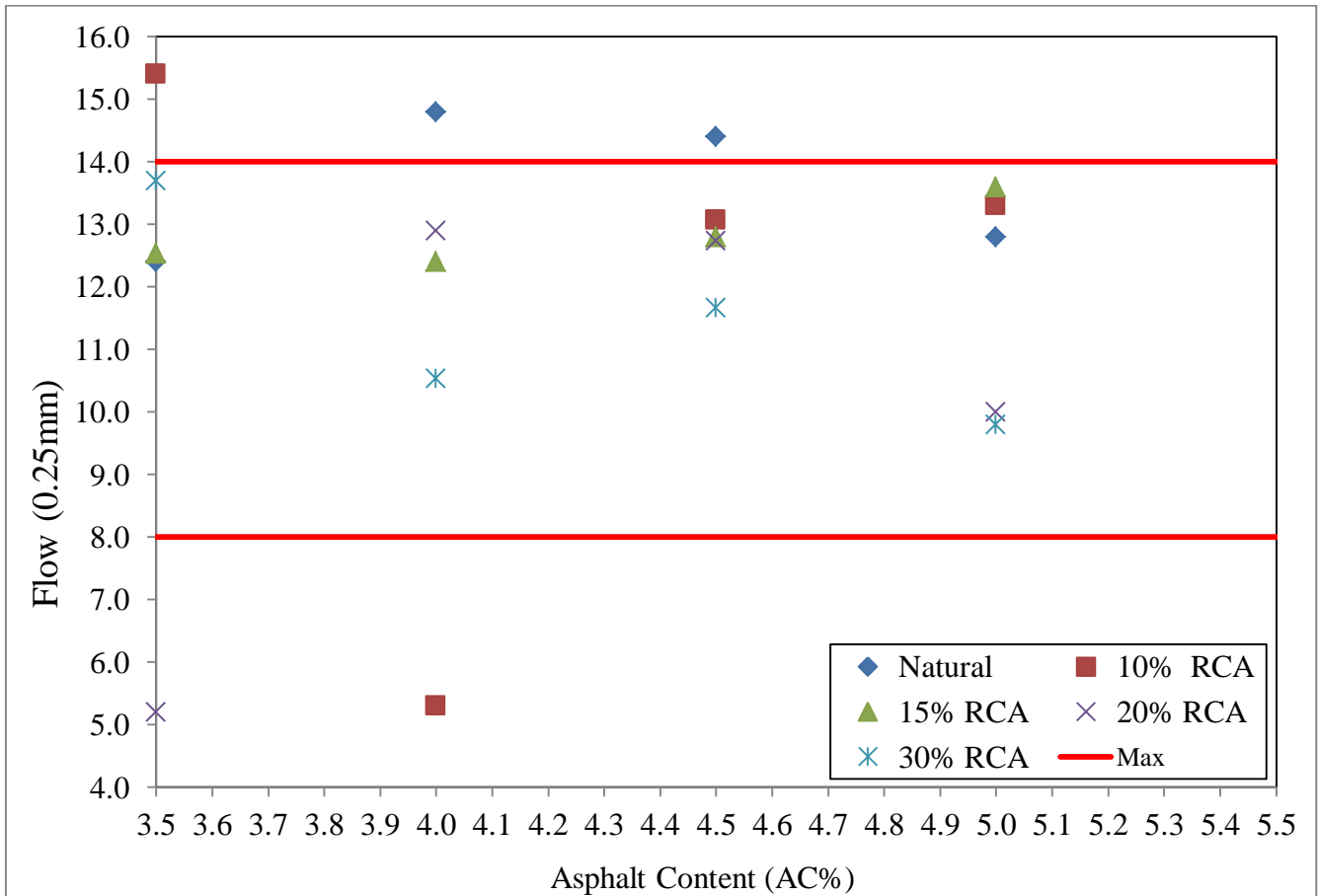


Figure 15 flow versus AC% for the five mixes

The results for the moisture sensitivity test shown in Table 15 show the increase in the TSR ratio when using 15% RCA indicating that using 15% fine RCA improves the mix when subjected to moisture. However, when using 30% fine RCA the mix didn't pass the minimum requirement of 80%. These results will be further explained in the section 4.4.

Table 15 IDT results, average Air voids of the tested specimens, and the corresponding TSR

Mix	Condition	Tensile Strength (KPa)	Average AV%	TSR
Control	Dry	1132.8	6.5	91
	Freeze-Thaw	1030.8	6.4	
15% RCA	Dry	975.0	6.9	105
	Freeze-Thaw	1022.9	6.6	
30% RCA	Dry	1238.0	6.5	<b>75</b>
	Freeze-Thaw	926.7	6.6	

### 4.3 Superpave Mix Design

#### 4.3.1 Optimum Asphalt Content Validation

Assuming that the optimum of a mix should not vary between the Marshall Mix design and the Superpave Mix design, Superpave samples were prepared to validate this AC% for the 5 mixes. Therefore, the AV% of the samples should be within this range  $4 \pm 0.2\%$ . For the 10%, 15%, 20%, and 30%, the optimum AC% taken was 4.3%. However, the actual results of the validation didn't conform to the expected range of AV% as shown in table 16. The AV% for 10%, 15%, and 20% were less than 4% indicating that the asphalt content of 4.3% is too high for these mixes. While the AV% of 30% was greater than 4% indicating that the amount of asphalt in the mix is insufficient. Therefore, when a new material such as RCA was introduced into the mix, Marshall Mix design was not able to predict the optimum asphalt content at small intervals with only 5% difference from a mix to the other. This was evident in the air voids graphs where an interchange in the value between the mixes was noted.

Table 16 Results of Superpave samples compacted at optimum AC% used from Marshall

Mix Type (%RC A)	%AC	Actual $G_{mb}$ at $N_{des}$	Avg. $G_{mb}$	$G_{sb}$	$G_{mm}$	Actual AV% at $N_{des}$	Avg. AV%	VMA	Avg. VMA	VFA	Avg. VFA
0	3.84	2.399	2.402	2.709	2.497	4.0	<b>3.8</b>	14.9	14.8	73.3	74.1
0	3.84	2.406				3.7		14.6		74.9	
10	4.3	2.390	2.390	2.682	2.456	2.7	<b>2.7</b>	14.7	14.7	81.6	81.7
10	4.3	2.390				2.7		14.7		81.8	
15	4.3	2.379	2.378	2.669	2.455	3.1	<b>3.2</b>	14.7	14.7	78.9	78.6
15	4.3	2.376				3.2		14.8		78.2	
20	4.3	2.367	2.365	2.656	2.452	3.5	<b>3.5</b>	14.7	14.8	76.4	76.1
20	4.3	2.364				3.6		14.8		75.8	
30	4.3	2.334	2.330	2.630	2.448	4.7	<b>4.8</b>	15.1	15.2	69.1	68.3
30	4.3	2.326				5.0		15.4		67.6	

#### 4.3.2 Superpave Optimum Asphalt Content

Using the previous results, Superpave provides an equation to estimate the optimum asphalt content to obtain a 4% air void at  $N_{des}$ . Using this equation, the optimum asphalt contents were calculated and samples were prepared at the new asphalt content. The prepared volumetric samples provided air voids close to 4% as shown in Table 17. Table 18 represents the results of the compacted samples to  $N_{max}$ , all the samples passed the Superpave criteria.

Table 17 Results of Superpave samples compacted at calculated AC%

% RCA	% AC	Actual Gmb at Ndes	Gsb	Gmm	Actual AV% at Ndes	Average AV%	Average VMA	Average VFA
10	3.9	2.393	2.682	2.490	3.9	4.0	14.3	72.3
	3.9	2.388			4.1			
15	4.0	2.378	2.669	2.480	4.1	4.0	14.4	71.9
	4.0	2.381			4.0			
20	4.2	2.366	2.656	2.464	4.0	3.9	14.6	73.1
	4.2	2.369			3.9			
30	4.7	2.345	2.630	2.441	3.9	3.9	15.0	73.8
	4.7	2.345			3.9			

Table 18 Results of Superpave samples compacted to Nmax

Mix Type (%RCA)	% AC	Actual G <sub>mb</sub> at N <sub>max</sub>	G <sub>mm</sub>	Actual AV% at N <sub>max</sub>	% G <sub>mm</sub> @ N <sub>ini</sub>	Requirement	Status	% G <sub>mm</sub> @ N <sub>ini</sub>	Requirement	Status
0	3.8	2.440	2.497	2.3	97.7	<98	passing	85.7	< 89	passing
10	3.9	2.426	2.490	2.6	97.4			84.8		
15	4	2.429	2.480	2.1	97.9			85.8		
20	4.2	2.413	2.466	2.2	97.8			85.6		
30	4.7	2.388	2.439	2.1	97.9			85.5		



### 4.3.3 Dynamic Modulus

Samples for each of the five mixes were tested for dynamic modulus; the results for each mix were compared at each temperature and frequency. The difference between the replicate results was set to 12%. For each mix, the results of the analyzed dynamic modulus data are plotted versus the reduced frequency along with the sigmoidal fit and the shift factor of each mix as shown in figure 17,18,19,20, and 21. In addition, for each mix the average dynamic modulus master curve was plotted, the data was averaged based on the same reduced frequency. The plots for each mix are shown in figure 22. The n value is defined as the slope of the straight line segment in master curve, and indicates the sensitivity of change in modulus with frequency of loading. The higher this n value, the greater the changes in modulus for a corresponding change in frequency or vehicle speed (Carpenter, 2007). The n-values shown in Figure 16 were calculated for each of the mixes. Adding RCA up to 20% to the mix decreased the n-value thus limiting the sensitivity of the mix as a whole.

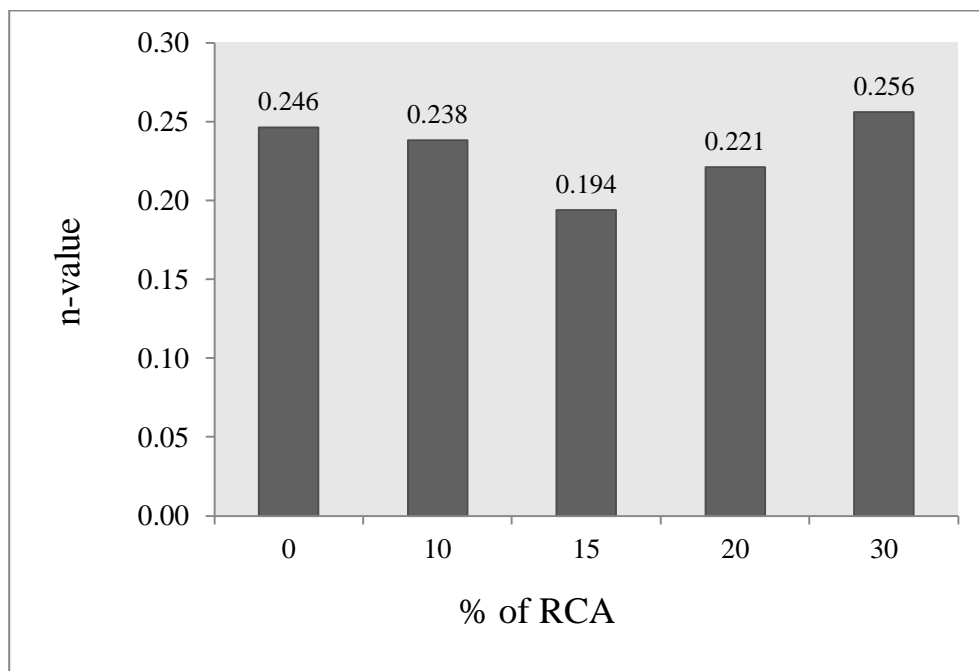


Figure 16 n-value versus %RCA in the mix

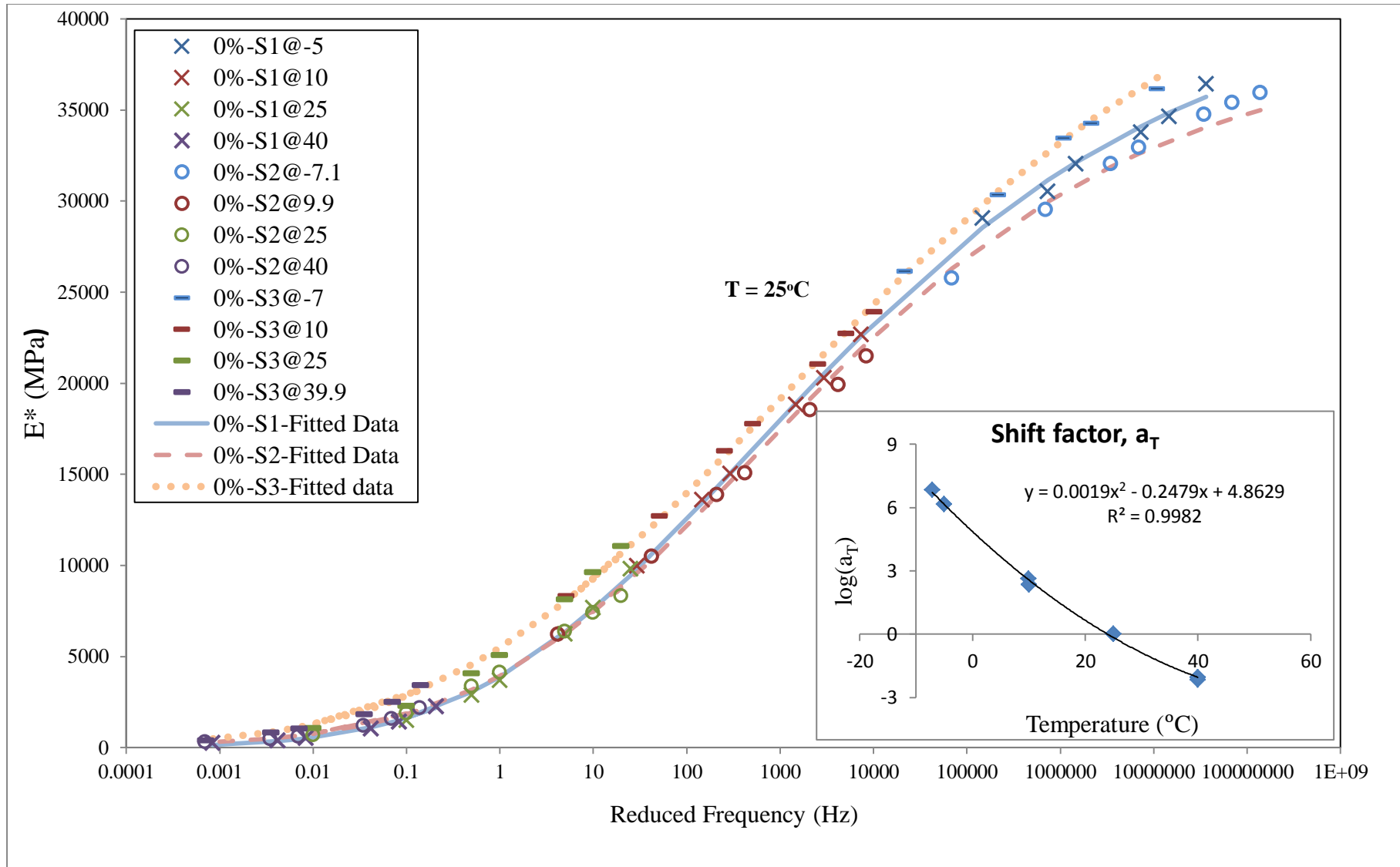


Figure 17  $E^*$  master curve for natural mixes at reference temperature - three replicates

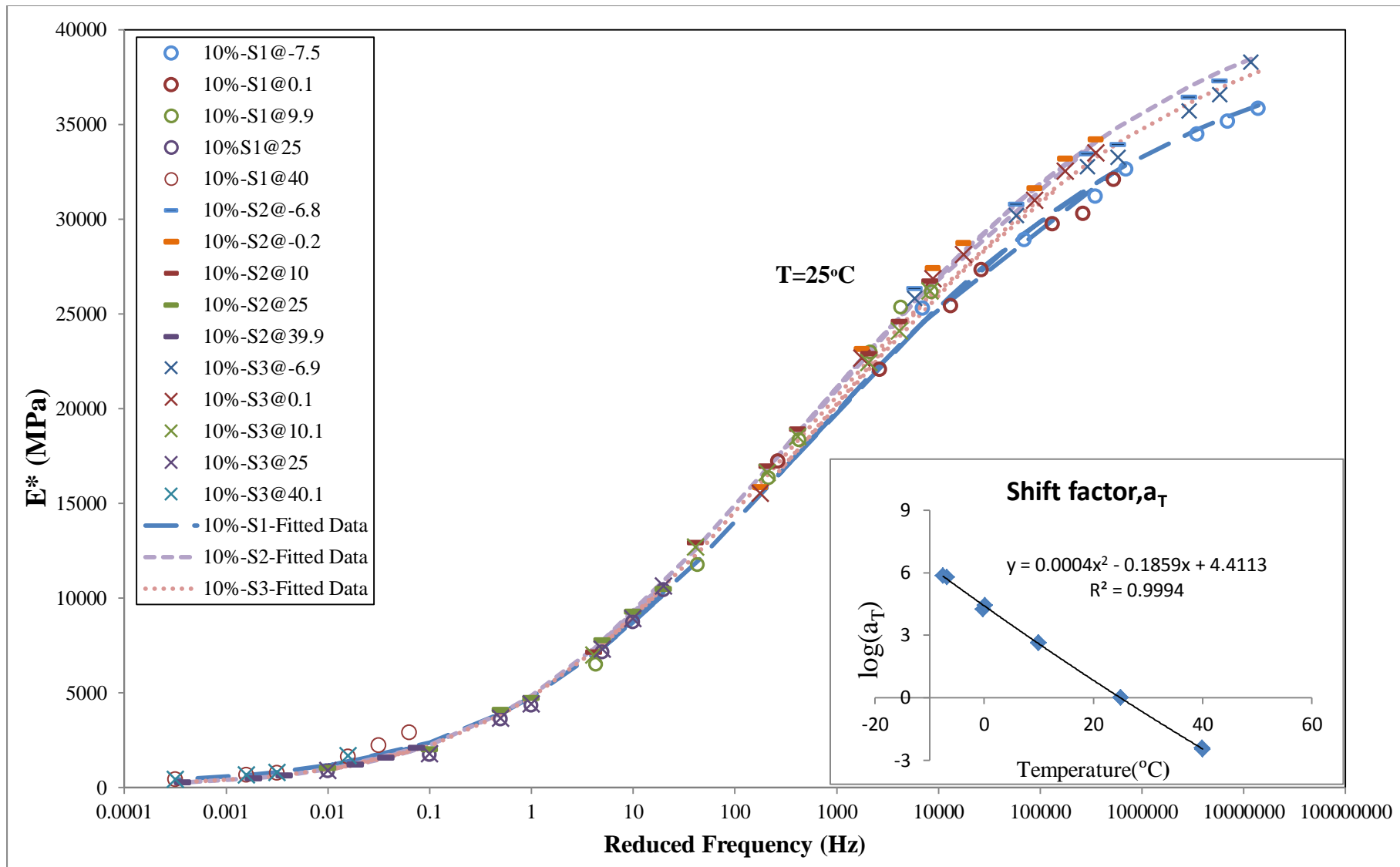


Figure 18  $E^*$  master curve for mixes with 10% RCA at reference temperature - three replicates

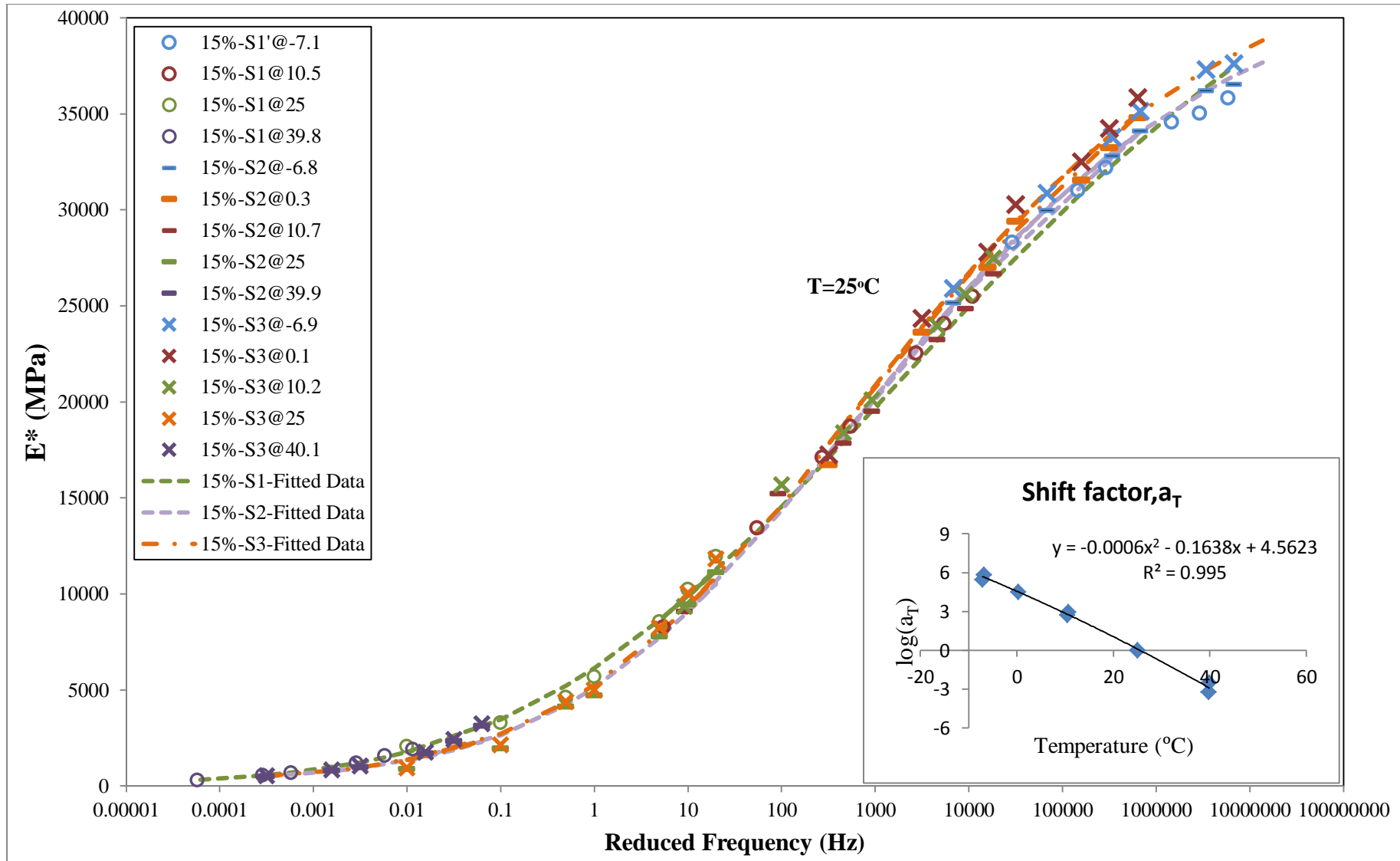


Figure 19  $E^*$  master curve for mixes with 15% RCA at reference temperature - three replicates

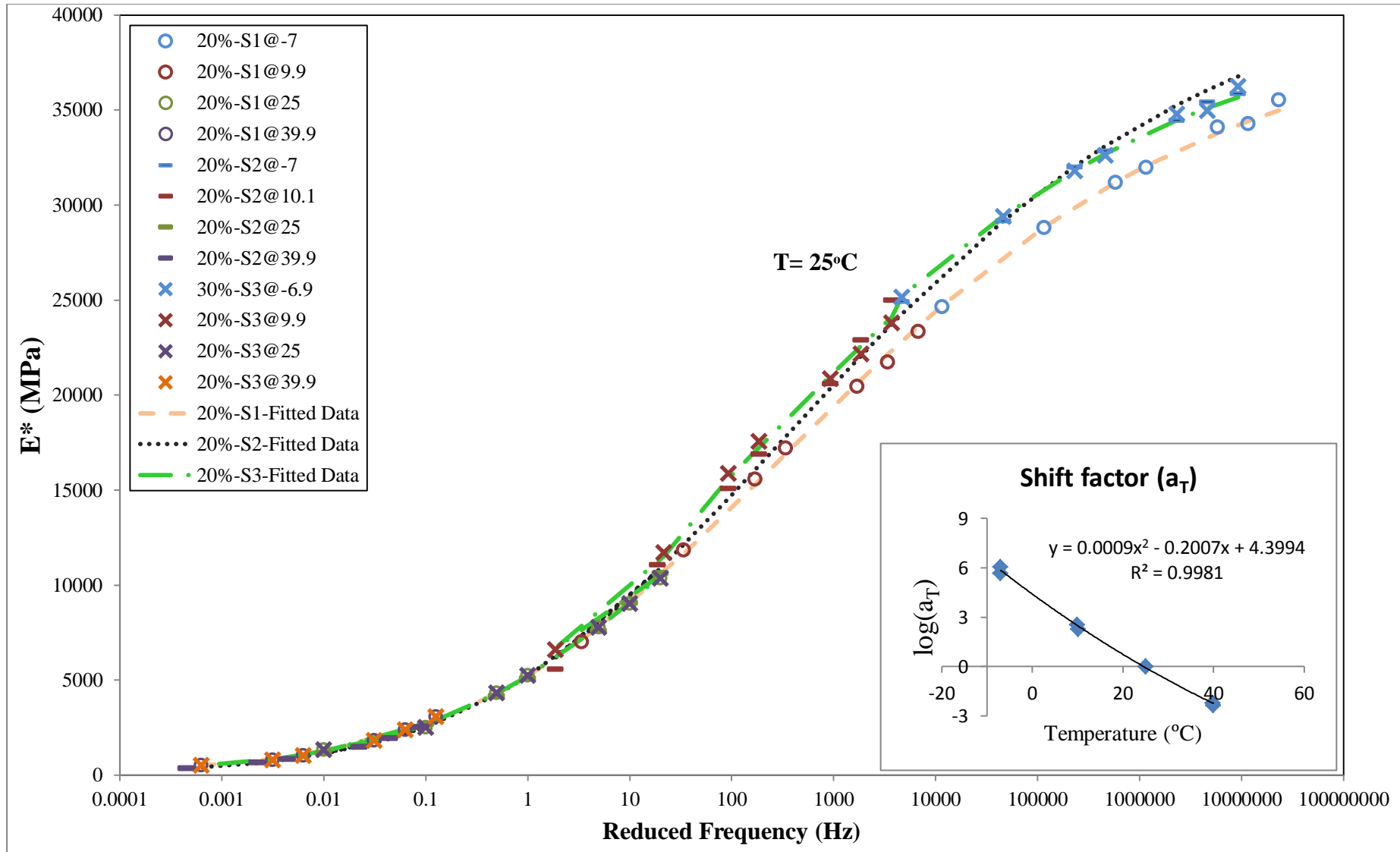


Figure 20  $E^*$  master curve for mixes with 20% RCA at reference temperature - three replicates

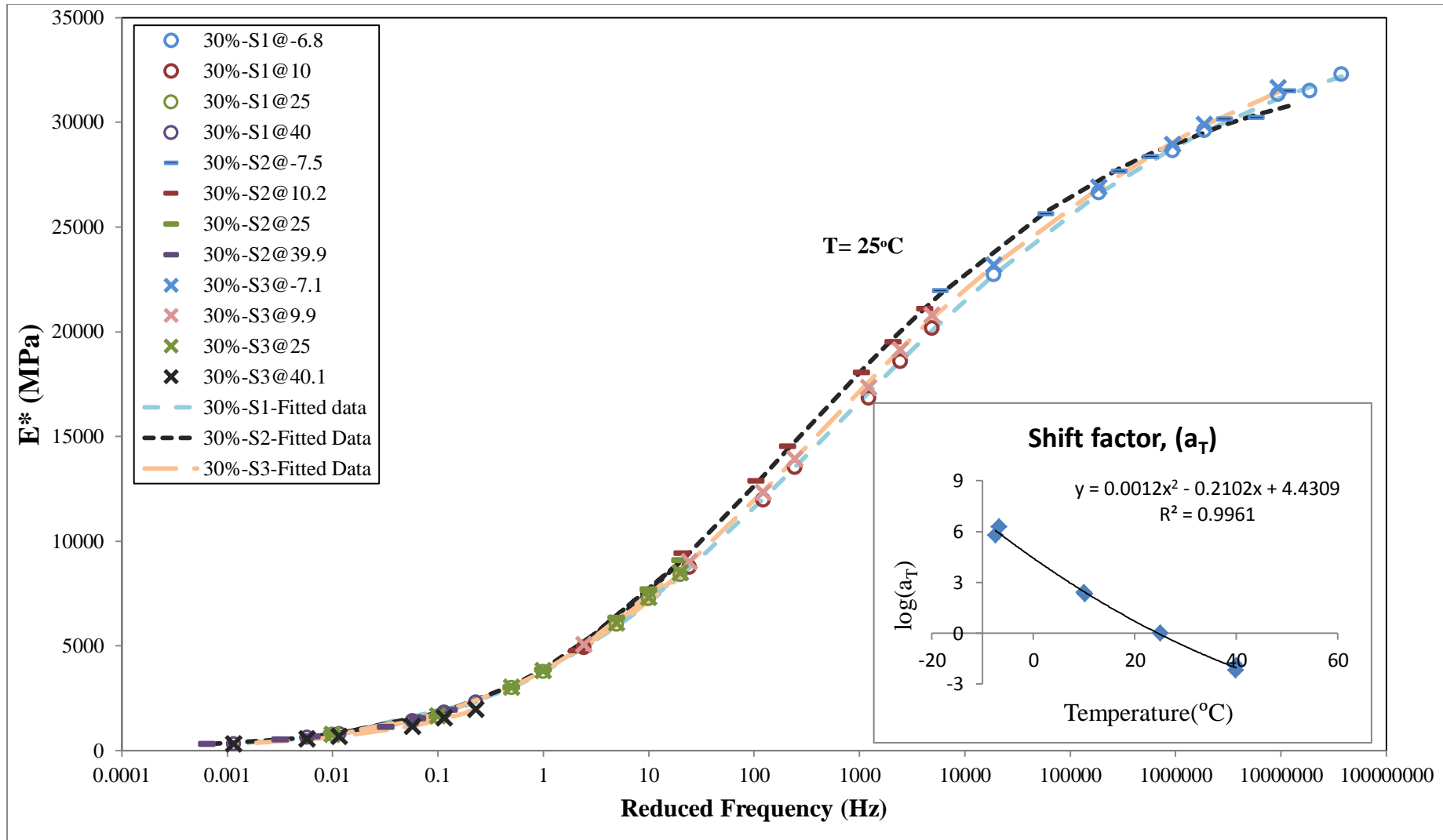


Figure 21  $E^*$  master curve for mixes with 30% RCA at reference temperature - three replicates

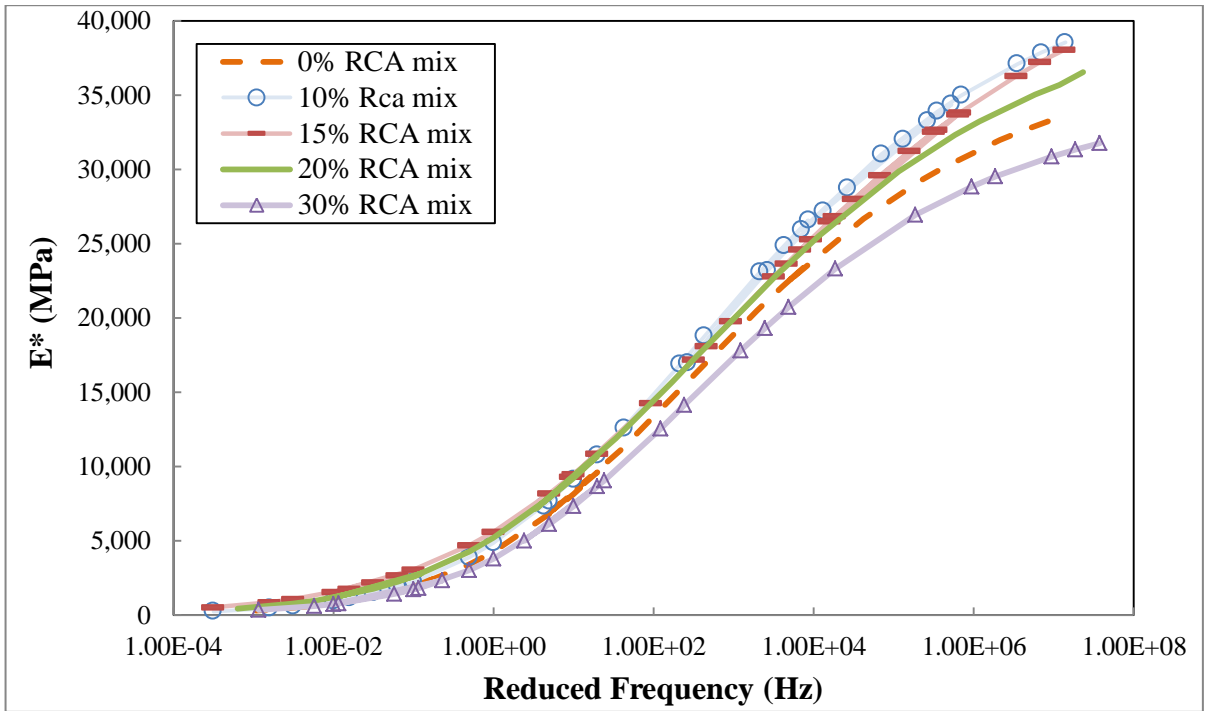


Figure 22 Average dynamic modulus master curves for mixes with different % of fine RCA

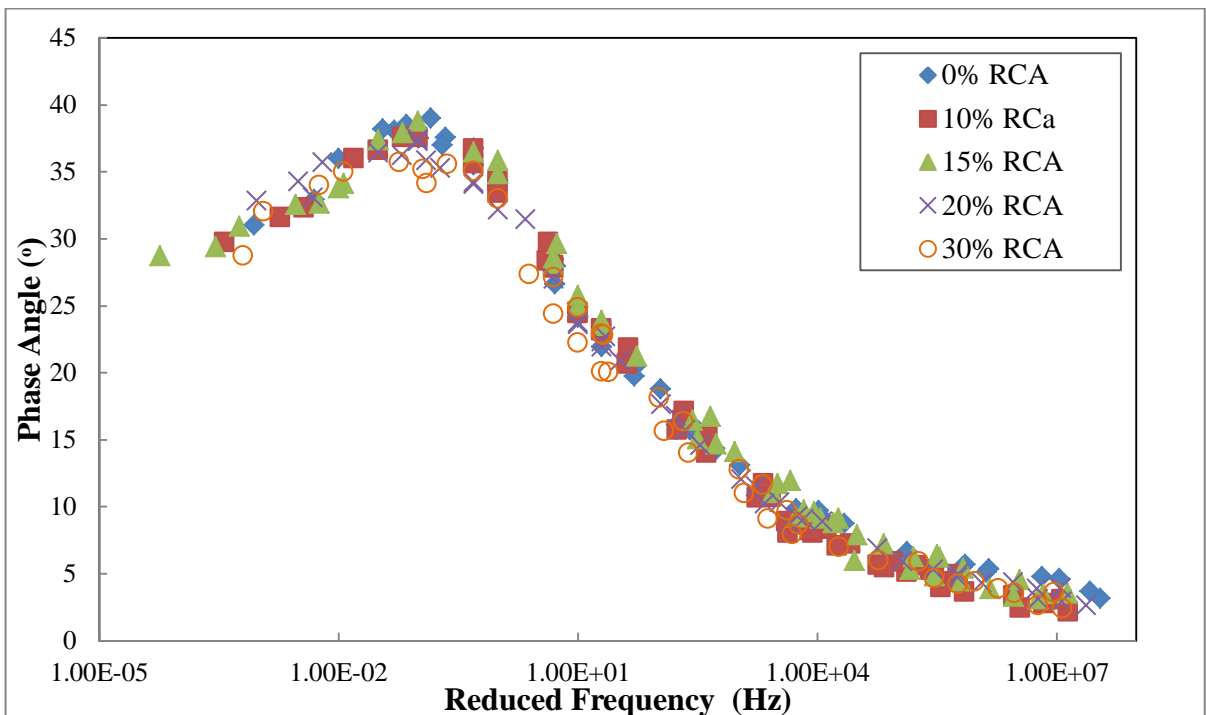


Figure 23 Phase angle master curves for mixes with different % of fine RCA

The master-curves at a reference temperature of 25°C for the average of the  $|E^*|$  and  $\delta$  are presented in Figure 22. It can be observed that the  $|E^*|$  curves appear to be overlapping for all the mixes at low reduced frequencies ( $f_r$ ). A deviation starts appearing at  $f_r$  higher than 1Hz where this difference increases with the increase in  $f_r$ . It is observed that the highest stiffness is obtained for RCA mix with 10% replacement. This stiffness decreases as the % of fine RCA in the mix increase up to 20% RCA replacement. Mixes with 30% fine RCA provide a lower stiffness than that of the control mix. Looking at the  $\delta$  curves shown in Figure 23 , mixes with RCA have no significant change on the  $\delta$  where the calculated values were in the vicinity of that of the control mix.

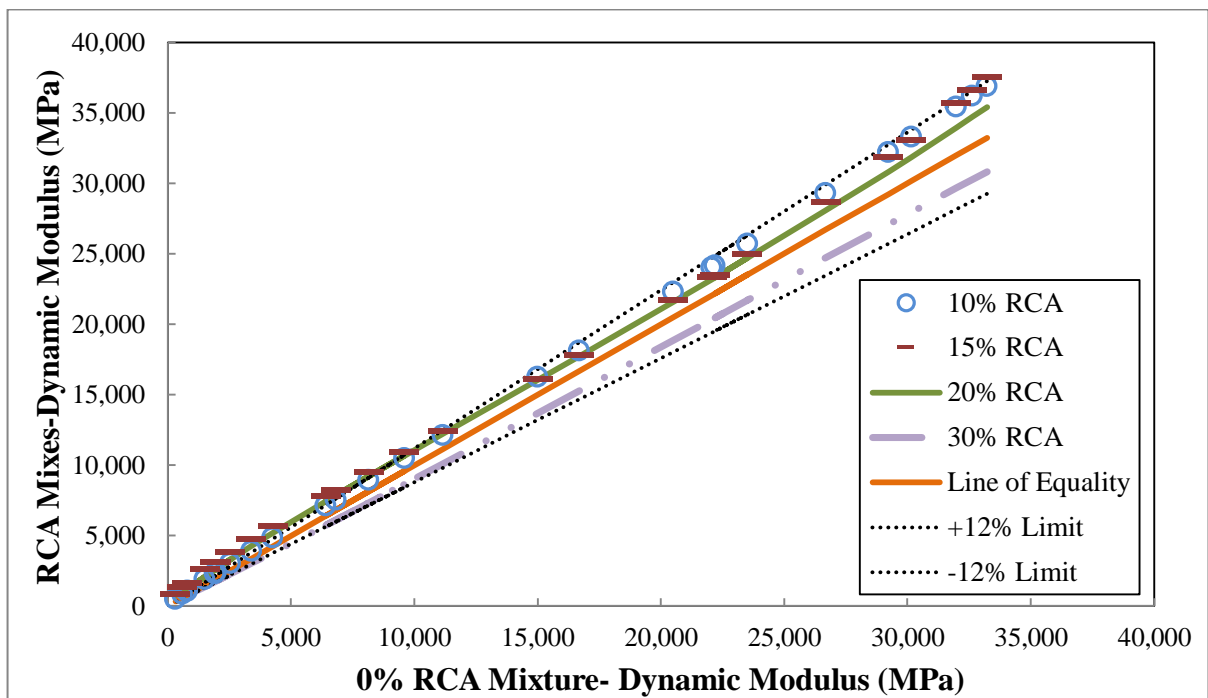


Figure 24 Comparison of mixes with fine RCA to the control mix

The comparison of the  $|E^*|$  of mixes with different percentages of fine RCA to the control mix is shown in Figure 24. The mixes were compared to the equality line which represents the  $|E^*|$  value of the control mix. In addition, the lower and upper limits were plotted to present  $\pm 12\%$  interval from this line. This interval was determined based on



the recommendation of AASHTO T342-11 which indicates that for three replicates with three LVDTs per each the estimated limit of accuracy is  $\pm 12\%$  of the true  $|E^*|$  of the mix. As shown in the figure, at high  $|E^*|$  values which correspond to high  $f_r$ , the four RCA mixes are within the 12% limits while at low  $|E^*|$  the RCA mixes slightly exceed these limits. It is observed that at high  $f_r$  (low temperature), mixes with 30% fine RCA have a stiffness lower than the control mix while 10% RCA mixes gave the highest stiffness. This indicates that this mix has the lowest thermal cracking resistance while that of 30% has the most thermal cracking resistance.

In order to assess the mixes, two temperatures will be considered 40°C and 25°C. HMA mixes are prone to rutting at high temperatures such as 40°C. In order for a mix to resist rutting, the dynamic modulus at such temperatures has to be high in addition the phase angle of the mix has to be low in order to exhibit elastic behavior. Therefore, in order to assess for rutting, a frequency of 0.1Hz will be considered. Based on literature, a rutting stiffness factor defined by  $E^*/\sin\phi$  can provide a better indicator for rutting at high temperature than the modulus alone, it can distinguish between a good and a poor mix (Bahia et al., 1994, Zhou et al., 2003, and Tashman and Elangovan, 2007). The dynamic modulus, the phase angle, and the rutting stiffness factor for each mix at 40°C and 0.1Hz are shown in Table 19.

Table 19 Ranking of the mixes based on the rutting stiffness factor

At 40°C at 0.1Hz					
% RCA	0	10	15	20	30
E*(Mpa)	297.8	345.2	401.5	429.5	327.2
Phase angle $\phi$ (°)	31.9°	31.4°	32.1°	33.7°	30.4°
$\sin(\phi)$	0.5565	0.5488	0.5608	0.5887	0.5300
Rutting Stiffness Factor $E^*/\sin(\phi)$	563.7	661.7	754.8	773.6	647.3
Ranking	5	3	2	1	4

Based on the obtained results, mixes with 20% RCA are the least prone to rutting. In addition, introducing 15%, 20%, and 30% RCA improves the rutting resistance of the mix.

Considering the 25°C, HMA mixes are prone to fatigue cracking. In order for a mix to resist fatigue cracking, the dynamic modulus and the phase angle at this temperature have to be low to ensure. An indicator for fatigue cracking would be loss modulus defined by  $E^*\sin\phi$  (Ye et al., 2009). The lower the loss modulus is the better the resistance to fatigue cracking. The dynamic modulus, the phase angle, and the fatigue stiffness factor for each mix at 25°C and 10Hz are shown in Table 20.

Table 20 Ranking of the mixes based on the fatigue stiffness factor

At 25°C at 10Hz					
% RCA	0%	10%	15%	20%	30%
E*(Mpa)	8187.3	8940.5	9480.6	9237.6	7333.6
Phase angle $\phi$ (°)	25.3	24.4	25.4	23.6	23.5
$\sin(\phi)$	0.4419	0.4266	0.4429	0.4127	0.4106
Fatigue Stiffness Factor E* $\sin(\phi)$	3501.1	3699.4	4063.0	3705.3	2927.0
Ranking	2	3	5	4	1

Based on the obtained results, mixes with 30% RCA are the least prone to fatigue cracking. The introduction of RCA up to 20% didn't improve the fatigue resistance. Up to a 30% of RCA in the mix is needed in order for the mix to be more elastic and thus less prone to fatigue.

#### 4.4 Mastic Testing

Typically, fillers are added to asphalt concrete mixes in order to stiffen the asphalt binder and enhance the mix's density and strength (Wang et al., 2011). Those fillers are fine powder particles passing sieve #200 and can be bag house fines, manufactured fillers, or recycled materials from industry wastes. RCA filler is investigated, as part of this study, to represent a type of filler that can be obtained from the recycling process of construction demolition wastes. Thus, different mastics were prepared to mimic the mastics found in the asphalt concrete mixes of this study as shown in Table 8. The properties of mineral fillers can influence the characteristics and performance of asphalt mastics and mixtures. Hence, RCA and limestone fillers will stiffen the asphalt mastic to different extents. This aspect is assessed using the Dynamic

Shear Rheometer through evaluating the viscosity, complex shear modulus, and multiple stress creep recovery (MSCR).

#### ***4.4.1 Viscosity***

As an indicator of the workability of the mastic which reflects on the constructability mix, viscosities of the different mastics were measured at different temperatures. It is a norm that the viscosity of a binder decreases with the increase in temperature; this is also applicable to mastics in which the binder softens with rising temperatures. The average apparent viscosity of the binder dropped down from 0.83 Pa.s to 0.24 Pa.s between 125°C and 150°C. These values increased to 2.8 Pa.s and 0.71 Pa.s upon adding the limestone filler. These results reflect the fact that filler stiffens the asphalt binder in a mix. However, for the same concentration of filler within mastic, as the percentage of limestone replaced with RCA filler increases the viscosity of the mastic increases. This increase in the viscosity of the mastic follows a trend at all temperatures for the 15% and 30% replacements where it increased from that of the limestone filler mastic by approximately 15% and 30%, respectively. Furthermore, for mastic containing only filler RCA, the viscosity increases by about three times than that of the mastic with limestone filler solely. In order to compare RCA filler with filler material from the literature, the viscosity ratio is calculated, which is the viscosity of the mastic at 135°C divided by the viscosity of the binder at 135°C also. The mastic containing only filler RCA has a viscosity ratio of 8 which is very high compared to different filler material and provides similar value when using soft filler granite (Wang et al., 2011).

To further investigate the effect of RCA versus limestone filler, it is notable that RCA is composed of limestone aggregates coated with mortar which is basically hydrated cement particles and sand. But, when RCA is crushed into filler it can be stated that the hydrated cement particles can break more easily and thus the RCA filler has much more hydrated cement particles than limestone powder. This can be explained by the compressive strength test done on limestone and concrete cubes presented earlier in this study where limestone was found to be about 2-3 times stronger than concrete. Thus, based on that a mastic sample was prepared using hydrated cement filler crushed from some cubes casted about 1 year earlier. This sample yielded a viscosity that is about 12% lower than that of mastic with RCA filler. The same was repeated with cement particles as a filler to check if the chemical elements present in cement have any effect on the viscosity knowing that cement is not commonly used as filler in HMA mixes. But, this yielded a viscosity that is exactly the same as that of the mastic with limestone filler. Thus, it can be concluded that the RCA filler can highly affect the workability of mastic compared to limestone filler. This can be due to the chemical composition of the RCA, the adhesive bond between the aggregate and the hydrated cement, or due to the different specific gravities of the fillers. Also, the larger surface area of the RCA filler might enhance the friction between the filler particles and the binder leading to the higher stiffening effect.

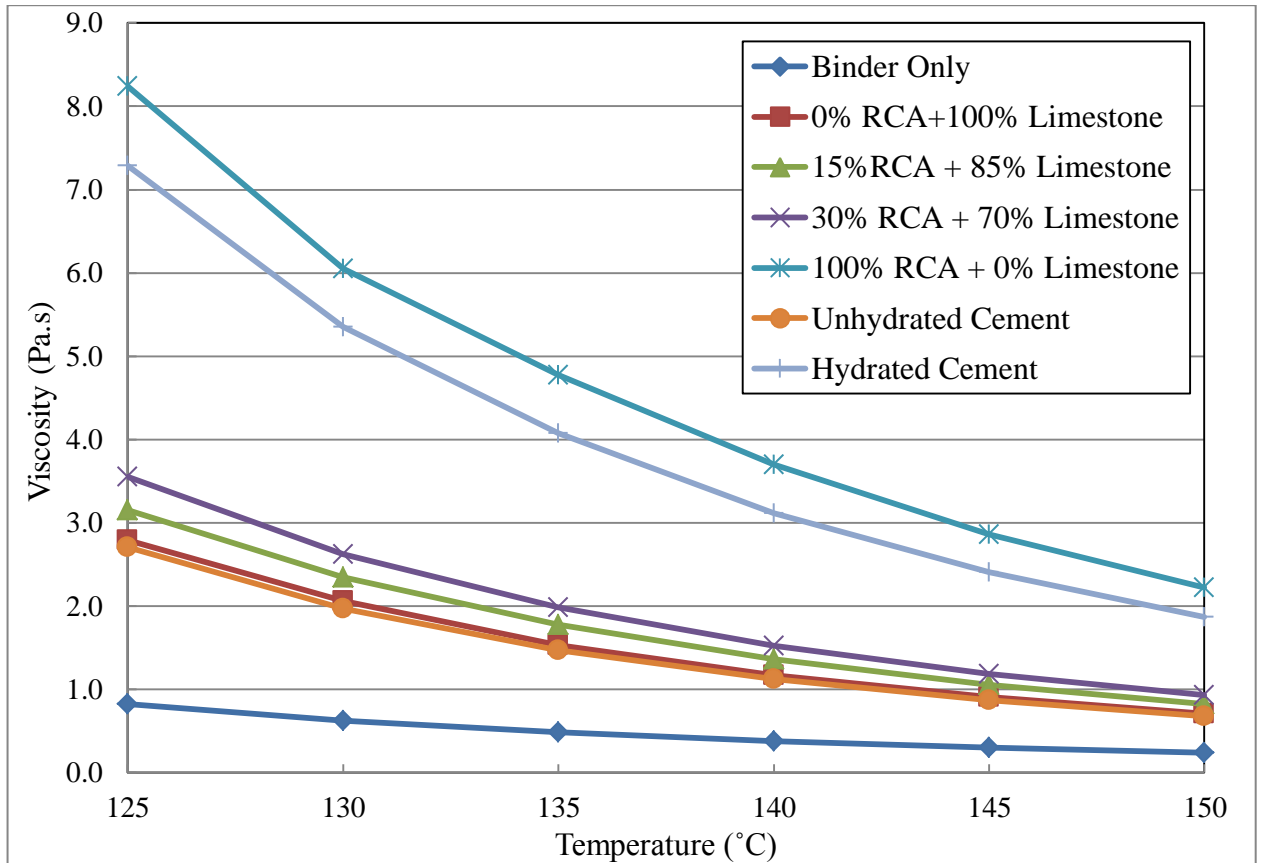


Figure 25 Viscosity values for each of the six mastics prepared

#### 4.4.2 Complex Shear Modulus and Phase angle

$G^*$  is used as an indicator for the stiffness of the mastic and its resistance to shear deformation under load. The results obtained for  $G^*/\sin\delta$  at 10 rad/sec present a trend similar to that of the measured viscosity with respect to the replacement of the limestone filler by RCA filler. The  $G^*/\sin\delta$  curve for a temperature range between 64°C and 88°C is shifted up by a factor of 2.5 when the filler used is limestone. This confirms the previous finding that the addition of filler is providing a stiffer binder in the asphalt mix. Upon the replacement of the limestone filler with RCA filler, the  $G^*/\sin\delta$  is shifted slightly upwards for diluted RCA concentrations of 15% and 30% and this curve is shifted by a factor of approximately 1.35 when the entire limestone filler is replaced with RCA. At low temperatures of 64°C, the  $G^*/\sin\delta$  value is high where it can be

explained that the binder is stiff and thus the effect of the filler is more dominant, but this manner is inverted as the temperature increases where the binder softens and thus it controls the properties of the mastic at high temperatures rather than the filler itself.

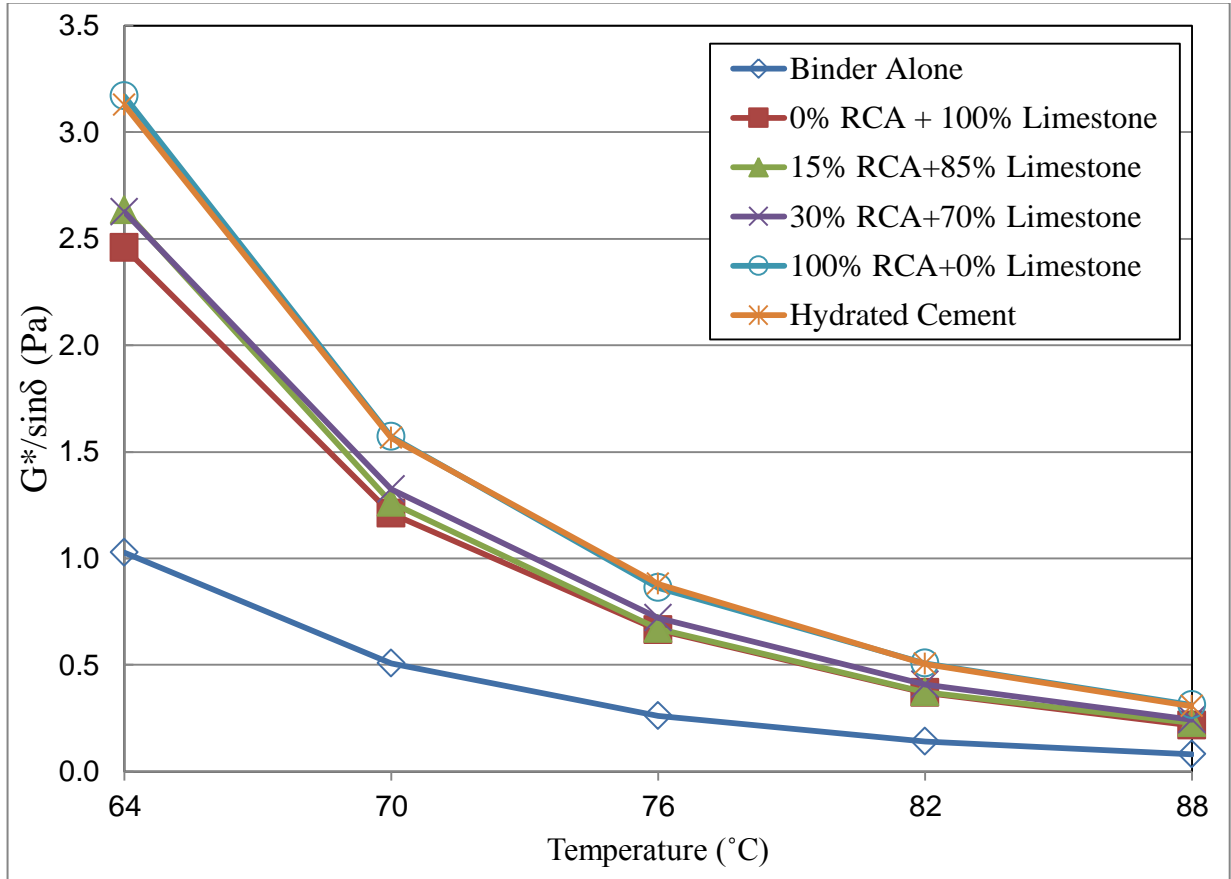


Figure 26  $G^*/\sin\delta$  at different temperatures for the 5 mastics prepared

The mastic with hydrated cement as a filler provides a  $G^*/\sin\delta$  value that is exactly the same as that of mastic with RCA filler. This supports the fact that most of RCA filler is composed of hydrated cement powder.

Taking  $G^*$  and  $\delta$  individually shows that the increase in value of  $G^*/\sin\delta$  upon addition of filler is explained by the stiffening of the binder body where  $G^*$  is significantly increased by the factor of 2.5 that is just mentioned. The mastic is more elastic than the binder itself due to the addition of aggregates which are elastic in nature.

The decrease in the value of  $\delta$  is  $1^\circ$  which indicates that the change in the mastic properties is due to the stiffening effect of the filler and not the elasticity. Moreover, the increase in the concentration of RCA filler increases  $G^*$  significantly; while  $\delta$  remains in the vicinity of  $87^\circ$  which indicates that there isn't a significant difference in the elasticity of RCA and limestone fillers. These results show that as the concentration of RCA filler increases, the mastic will be able to provide a better resistance to rutting at high temperatures.

The results of the  $G^*$  for the mastics containing 15% and 30% RCA filler can explain the stability results. Since  $G^*$  increase as the RCA filler in the mastic increases, this indicates that the failure in stability is not due to the mastic. Therefore, at 30% RCA replacement in the mix, the weakening factor is the fine RCA aggregates that are more dispersed in the mix at 30% RCA and cause the decrease in stability. Moreover, these results can also help explain the obtained moisture results the increase in  $G^*$  of the mastic helped in improving the TSR ratio of the mix at 15% RCA. However, the TSR ratio decreased when the fine RCA in the mix reached 30% this is solely due to the high amount of fine RCA in the mix that might have weakened the adhesive bonds when subjected to water.

The  $E^*$  master curves followed a trend where by 10% RCA had the highest curve followed with the 15% RCA, the 20% RCA, the natural mix and the 30% RCA mix being the lowest. Introducing fine RCA into the mix generally increases the  $E^*$  values and this can be attributed to the mastic that becomes stiffer. On the other hand, as the percentage of fine RCA in the mix increases the  $E^*$  values start to shift downward. At 30% RCA, even though the mastic is the strongest the amount of fine RCA cause the  $E^*$  values to decrease below those of the natural mix.



#### 4.4.3 Multiple Stress Creep and Recovery (MSCR)

Another measure considered to study the reactivity of the filler with the binder is the non-recoverable creep compliance ( $J_{nr}$ ) measured in DSR with parallel plate geometry by the multiple stress creep recovery test. This test method determines the presence of elastic response in the studied mastics where the creep portion of the test lasts for 1 second followed by a 9 seconds period of recovery for 10 consecutive cycles for each of the stress levels used: 0.1 kPa and 3.2 kPa at 64°C. The  $J_{nr}$  at 0.1 kPa can be considered as an indicator of the properties in the linear viscoelastic region; while, the  $J_{nr}$  at 3.2 kPa will be taken as an indicator of rutting susceptibility.

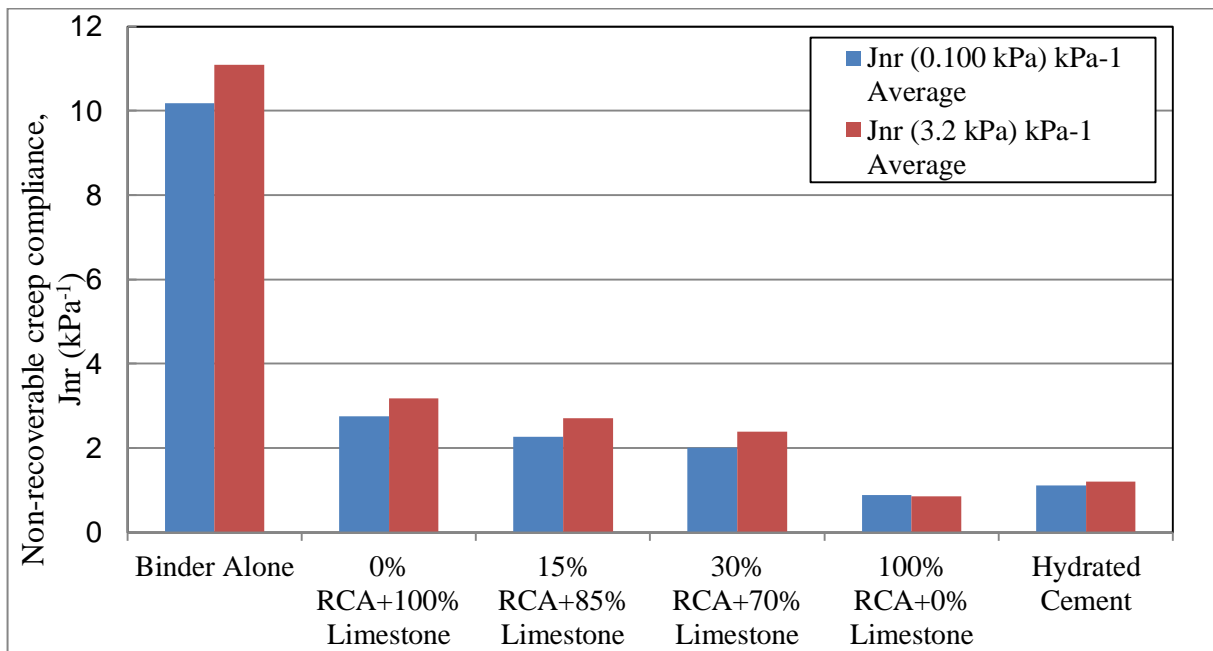


Figure 27  $J_{nr}$  results for the five mastics

The results for  $J_{nr}$  at 0.1 kPa are observed to be similar to those of  $G^*/\sin\delta$  where  $J_{nr}$  at 0.1 kPa dropped from  $10.2 kPa^{-1}$  to  $2.8 kPa^{-1}$  when the mastic contains limestone which is approximately a drop by a factor of 3.5. This value continues to decrease with the increase of the % of replacement of limestone by RCA to reach a minimal value of

0.9 kPa<sup>-1</sup> when the entire filler is constituted of RCA. Thus the use of RCA allows the mastic to have a higher recovery at low stress level.

The trend of  $J_{nr}$  at 3.2 kPa is similar to that at 0.1 kPa; knowing that  $J_{nr}$  at 3.2 kPa is always higher than that at 0.1 kPa because the higher level of stress leads to more damage in the mastic. But, it is remarkable here that filling the binder reduced the  $J_{nr}$  by a factor of 3.5 times for limestone implying that the filler plays a significant role in providing more resistance to permanent deformation.

For the case of mastic with only RCA filler,  $J_{nr}$  at 3.2 kPa is approximately the same as that at 0.1 kPa taking three replicates into consideration. This shows that RCA as a filler is able to stiffen the binder enough so that it will have high rutting resistance. So, this mastic is stiff enough and it has the same behavior at low and high stress levels where it is still in the linear viscoelastic range unlike other types of mastics presented in this study. Based on this, RCA can be recommended as filler for HMA mixes that will be placed in hot conditions with slow traffic in order to resist the ability of these mixes to rut.

## CHAPTER 5

### CONCLUSIONS AND FUTURE WORK

#### 5.1 Conclusions

This research study investigated the use of RCA in HMA as a replacement percentage of fine natural aggregates. The following conclusions can be drawn from the obtained study results:

- Using Marshall mix design method showed several drawbacks when it comes to properly identifying the different optimum asphalt content for added new material such as RCA. According to this method 10%, 15%, 20%, and 30% have a close asphalt content of 4.3% which was disproved using Superpave mix design.
- The optimum asphalt content obtained from Marshall is not representative of the optimum asphalt content for the Superpave mix.
- Superpave design properly showed the difference in optimum asphalt content between RCA mixes at small percentage replacement.
- According to stability results, using fine RCA up to 30% yields a higher stability than the natural mix. However, to ensure that the mix performs at its highest stability levels on all asphalt contents the limit of RCA usage should be 20%.
- The replacement of 15%, 20% and 30% RCA improved the rutting resistance of the mix; 20% being the mix least prone to rutting.
- The replacement of 30% RCA improved the fatigue resistance of the mix.

- The use of different percentage replacement of RCA as a filler improves the complex shear modulus and improves the non-recoverable creep compliance.
- The use of 100% RCA filler provides the same non-recoverable creep compliance at stress levels of 0.1Kpa and 3.2 Kpa indicating it provides high resistance to rutting.

## **5.2 Future Work**

The introduction of fine RCA as a replacement of fine natural aggregate has shown to provide acceptable performance. The idea of incorporating RCA in HMA is thus a valid concept towards producing more sustainable HMA mixes. However, several areas are still to be further investigated. The following are the recommended for future research:

- Investigating HMA mixes using only RCA filler in order to better understand the effect of RCA filler on the mix. The findings from this study might allow the adoption of the use of RCA as filler in HMA.
- Conducting further testing on the RCA mixes such as flow number test, indirect tensile test, and moisture sensitivity study on Superpave samples
- Investigating different sources of RCA in order to ensure that the source doesn't affect the obtained results and still can provide results better than the natural mix.
- Conducting life cycle assessment of using RCA in order to understand the true value that the use of RCA will have on the environment

## REFERENCES

- ACI committee-555 Report, (2001). "Removal and Reuse of Hardened Concrete."
- Anderson, K.W., Uhlmeyer, J. S., & Russell, M. A. (2009). "Use of Recycled Concrete Aggregate in PCCP: Literature Search" (No. WA-RD 726.1).
- Arabani, M., and Azarhoosh, A.R. (2012). "The effect of recycled concrete aggregate and steel slag on the dynamic properties of asphalt mixtures". *Construction and Building Materials Vol. 35, 1-7*.
- Aziz Memon, N. (2006). "Comparison between Superpave gyratory and Marshall laboratory compaction methods". Doctoral dissertation, Universiti Teknologi Malaysia, Faculty of Civil Engineering.
- Bahia, H.U., D.A. Anderson, D.W. Christensen, R. Dongre & M.G. Sharma, C.C. Antle, & J. Button (1994). "Binder Characterization and Evaluation, Vol. 3; Physical Characterization. SHRP A-396". Strategic Highway Research Program, National Research Council, Washington, DC.
- Bassan, M., and Quattrone, M. (2013). "Progress of Recycling in the Built Environment: Final Report of the RILEM Technical Committee 217-PRE". (Vol. 8), chapter 3.6. Springer.
- Burton, I. (1987). Report on Reports: Our Common Future: The World Commission on Environment and Development. Environment: Science and Policy for Sustainable Development, 29(5), 25-29.
- Button, J. W., Little, D.N., Jagadam, V., and Pendelton, O.J.(1994) "Correlation of Selected Laboratory Compaction Methods with Field Compaction". Transportation Research Record 1454, TRB, National Research Council, Washington, D.C., July 1994, pp 193-201.
- Carlberg, M., Berthelot, B., & Richardson, N. (2003). "Comparison of Marshall and Superpave gyratory volumetric properties of saskatchewan asphalt concrete mixes". Superpave Implementation and Experience in Canada, 5.
- Carpenter, S. H. (2007). "Fatigue performance of IDOT mixtures."
- Caro, S., Masad, E., Bhasin, A., & Little, D. (2009). "Coupled micromechanical model of moisture-induced damage in asphalt mixtures". Journal of Materials in Civil Engineering, 22(4), 380-388.

- Chehab G.R. (2002). "Characterization of Asphalt Concrete in Tension Using a Viscoelastoplastic Model", Ph.D. Dissertation, North Carolina State University, Raleigh, NC.
- Choubane, B., Page G., and Musselman, J. (2000). "Effects of Different Water Saturations Levels on the Resistance of Compacted HMA Samples to Moisture Induced Damage". Transportation Research Record 1723, Washington, D.C., pp. 97-106.
- Cho, Y.H., Yun, T., Kim, I.T., and Choi, N.R.(2011). "The application of Recycled Concrete Aggregate (RCA) for Hot Mix Asphalt (HMA) base layer aggregate." KSCCE Journal of Civil Engineering 15.3 (2011): 473-478.
- Corinaldesi, V., and Moriconi, G. (2004). "Concrete and mortar performance by using recycled aggregates." Construction Demolition Waste, Proceedings of the two-day International Conference, Concrete and Masonry Group within the School of Engineering at Kingston University, 157-164.
- Evangelista, L., & De Brito, J. (2007). "Mechanical behavior of concrete made with fine recycled concrete aggregates". Cement and Concrete Composites, 29(5), 397-401.
- Fabiana da Conceição Leite, Rosângela dos Santos Motta, Kamilla L. Vasconcelos, Liedi Bernucci,(2011). "Laboratory evaluation of recycled construction and demolition waste for pavements". Construction and Building Materials, Volume 25, Issue 6, June 2011, Pages 2972-2979.
- Faheem, A. F., & Bahia, H. U. (2010). "Modelling of asphalt mastic in terms of filler-bitumen interaction". Road Materials and Pavement Design, 11(sup1), 281-303.
- FHWA-Federal Highway Administration(2004): "Transportation Applications of Recycled Concrete Aggregate: FHWA State of the Practice National Review September 2004. National Review".US Department of Transportation and Federal Highway Administration, Washington, DC.
- Fromm, H. J. (1974). "The Mechanisms of Asphalt Stripping from Aggregate Surfaces". *Proc., Association of Asphalt Paving Technologists*, Vol. 43, pp. 191–223.
- Herrador, Rosario, et al. (2011) "Use of Recycled Construction and Demolition Waste Aggregate for Road Course Surfacing." *Journal of Transportation Engineering* 138.2 : 182-190.
- Jiqing Zhu, Shaopeng Wu, Jinjun Zhong, Dongming Wang,(2012). "Investigation of asphalt mixture containing demolition waste obtained from earthquake-damaged buildings". *Construction and Building Materials*, Volume 29, April 2012, Pages 466-475.

- John, V and Angulo, S. (Ed.). (2013). "Progress of Recycling in the Built Environment: Final Report of the RILEM Technical Committee 217-PRE" (Vol. 8), chapter 2.1. Springer.
- Julian Mills-Beale, Zhanping You,(2010). "The mechanical properties of asphalt mixtures with Recycled Concrete Aggregates".Construction and Building Materials, Volume 24, Issue 3, March 2010, Pages 230-235.
- Kiggundu, B. M., and Roberts, F. L. (1988). "Stripping in HMA mixtures: State-of-the-art and critical review of test methods." National Center for Asphalt Technology (NCAT), Auburn, Alabama. Rep. No. NCAT 88-02,
- Kim, Y. R., D. N. Little, and R. L. Lytton. (2002). "Fatigue and Healing Characterization of Asphalt Mixtures". *Journal of Materials in Civil Engineering*, American Society of Civil Engineers.
- Liang, R. Y. (2008). "Refine AASHTO T283 Resistance of Compacted Bituminous Mixture to Moisture Induced Damage for Superpave". Federal Highway Administration State Job Number: 134221
- Little, D. N., & Jones, D. R. (2003). "Chemical and mechanical processes of moisture damage in hot-mix asphalt pavements." National seminar on moisture sensitivity of asphalt pavements (pp. 37-70). California: San Diego
- McCann, M. and Sebaaly, P. (2001). "A Quantitative Evaluation of Stripping Potential in Hot Mix Asphalt Using Ultrasonic Energy for Moisture Accelerated Conditioning". Transportation Research Record 1767, Washington, D.C., pp. 48 – 59.
- Majidzadeh, K., and F. N. Brovold. (1968)." *Special Report 98: State of the Art: Effect of Water on Bitumen–Aggregate Mixtures*". HRB, National Research Council, Washington, D.C.
- Mishulovich, A (2003). "Used concrete/construction debris in Portland cement manufacturing". Portland Cement Association Research and Development Report Serial No. 2635
- Nixon, P. J. (1978). "Recycled concrete as an aggregate for concrete—a review". *Matériaux et Construction*, 11(5), 371-378.
- Neville, A. M., (1995). "Properties of concrete", 4th ed., London, Longman.
- Pérez, I., A. R. Pasandín, and J. Gallego, (2012). "Stripping in hot mix asphalt produced by aggregates from construction and demolition waste". *Waste Management & Research*, Volume 30.1 , January 2012, Pages 3-11.

- Pérez, A.R. Pasandín, L. Medina (2011). "Hot mix Asphalt Using C&D Waste as Coarse Aggregates". *Materials & Design*, Volume 36, April 2011, Pages 840-846.
- Rebuild Lebanon (2008). "Lebanon Reconstruction: Progress and Challenges". Presidency of the Council of Ministers.
- Srouf, I. M., Chehab, G. R., & Gharib, N. (2012). "Recycling construction materials in a developing country: four case studies". *International Journal of Engineering Management and Economics*, 3(1), 135-151.
- Srouf, I. M., Chehab, G., El-Fadel, M., & Tamraz, S. N. (2013). "Pilot-based assessment of the economics of recycling construction demolition waste." *Waste Management & Research*.
- Stroup-Gardiner, M., & Wattenberg-Komas, T. (2013). "Recycled Materials and Byproducts in Highway Applications". Volume 6: Reclaimed Asphalt Pavement, Recycled Concrete Aggregate, and Construction Demolition Waste. NCHRP Synthesis of Highway Practice, 6(Project 20-05, Topic 40-01).
- Sumeda Paranavithana, Abbas Mohajerani,(2006). "Effects of recycled concrete aggregates on properties of asphalt concrete". *Resources, Conservation and Recycling*, Volume 48, Issue 1, Pages 1-12.
- Tashman, L., and Elangovan, M. A. (2008). "Dynamic Modulus Test-Laboratory Investigation and Future Implementation in the State of Washington" (No. WA-RD 704.1).
- Terrel, R. L., and J. W. Shute. (1989). "*Summary Report on Water Sensitivity.*" SHRP-A/IR-89-003. Strategic Highway Research Program, National Research Council, Washington, D.C.
- Terrel, R. L., and S. Al-Swailmi. (1994)."*Water Sensitivity of Asphalt-Aggregate Mixes: Test Selection.*". SHRP Report A-403. Strategic Highway Research Program, National Research Council, Washington, D.C.
- Uche, O. A. U. (2008). "Influence of Recycled Concrete Aggregate (RCA) on Compressive Strength of Plain Concrete". *Pan, Continental J. Engineering Sciences*.
- UNRWA (United Nations Relief and Works Agency) (2008), "A Common Challenge A Shared Responsibility." The International Donor Conference for the Recovery and Reconstruction of the Nahr el-bared Palestinian Refugee Camp and Conflict-Affected Area of North Lebanon, Vienna, Austria.
- Vavrik, W. R., Huber G., Pine, W. J., Carpenter, S. H., and Bailey, R. (2002). "Bailey Method for Gradation Selection in Hot-Mix Asphalt Mixture Design".



Transportation Research E-Circular, Transportation Research Board, Washington D.C., No. E-C044.

Vázquez, E. (Ed.). (2013). "Progress of Recycling in the Built Environment: Final Report of the RILEM Technical Committee 217-PRE". (Vol. 8). Springer.

Von Quintus et al.(1989). "Comparative Evaluation of Laboratory Compaction Devices Based on Their Ability to Produce Mixtures with Engineering Properties similar to those produced in the Field,". Transportation Research Record 1228, TRB, National Research Council, Washington, D.C.

Vrijders, J. and Desmyter, J . (Ed.). (2013). "Progress of Recycling in the Built Environment: Final Report of the RILEM Technical Committee 217-PRE". (Vol. 8), chapter 3.1. Springer.

Wang, H., Al-Qadi, I. L., Faheem, A. F., Bahia, H. U., Yang, S. H., & Reinke, G. H. (2011). Effect of mineral filler characteristics on asphalt mastic and mixture rutting potential. *Transportation Research Record: Journal of the Transportation Research Board*, 2208(1), 33-39.

Witczak, M., Kaloush, K., Pellinen, T., El-Basyouny, M., and Von Quintus, H. (2002). "Simple Performance Test for Superpave Mix Design". NCHRP Report 465, National Cooperative Highway Research Program, Transportation Research Board.

Ye, Q., Wu, S., & Li, N. (2009). "Investigation of the dynamic and fatigue properties of fiber-modified asphalt mixtures". *International Journal of Fatigue*, 31(10), 1598-1602.

## APPENDIX-A

### EXPERIMENTAL PROCEDURE

This section below will explain the procedure followed in order to prepare Marshall and Superpave HMA samples.

#### *A.1 Sieving*

- 1- Check that the sieves are clean and that no material is retained in it.
- 2- Check that the sieves are arranged in the right order from smallest to largest ( Pan- #200 - #100 - #50 - #30 - #16 - #8 - #4 -  $\frac{3''}{8}$  -  $\frac{1''}{2}$  -  $\frac{3''}{4}$  - 1'' ).
- 3- Place two scoops of aggregates in the sieve shaker when using the small sized sieve (8'' diameter) and three scoops of aggregates when using the large sized sieve (12'' diameter). Tighten the screws and turn the shaker on for 15 min.
- 4- When done, remove the sieved material from each sieve and place it in its respective bucket. Make sure to close the bucket so that the sieved material remains intact.
- 5- Make sure to clean the sieve between the samples to ensure effective sieving. Keep repeating the above steps in order to obtain the weight needed from each sieve size.

#### *A.2 Batching*

There are four types of samples to be batched for this study : volumetric 4'' compacted sample for Marshal Mix design (1200g), volumetric 6'' compacted sample for Superpave Mix design (4700g) , dynamic modulus 6'' compacted sample (ranging

between 6950g and 7200 g depending on the mix), and loose mix sample for determining theoretical maximum specific gravity (1750g).

- 1- Depending on the mix to be batched, choose the appropriate size of the bowl.
- 2- Make sure the bowl is clean and dry.
- 3- Make sure the balance (capacity: 12kg, sensitivity: 0.1g) used is leveled, has a clean surface and that no weight is attached to the balance from the bottom. Note that a different balance can be used as long as the sensitivity is 0.1g and the capacity is greater than the sample to be batched.
- 4- Place the bowl on the balance, record its weight and then zero the balance.
- 5- From the previously sieved aggregates, add the needed amount of each aggregate size as shown on the batching sheet.
- 6- Make sure to add each size in a pile so that in case excess amount of aggregates is added, it can be easily removed to obtain the desired weight.
- 7- Zero the balance and add all the aggregate sizes needed according to the batching sheet.
- 8- When done, remove the mix, zero the balance and record the total weight of the mix and the bowl. Calculate the weight of the mix. The obtained value should not vary more than  $\pm 0.5g$  from the desired batch weight.
- 9- Cover the bowl with aluminum foil and label the mix with its number.

### ***A.3 Mixing***

- 1- Place the batched mixes, the mixing bowl, whip and spoons in the oven overnight at a temperature 10°C higher than mixing temperature (175°C).

- 2- Before 2 hours from the beginning of mixing, place the previously filled asphalt cans in the oven at 165°C. Make sure that the required temperature is met before starting to mix.
- 3- Remove the mix and place it on the balance. Make sure to zero the balance
- 4- Mix the aggregates with a heated spoon and add the required amount of asphalt for the mix; use a paper towel to extract the excess amount of asphalt if more is added
- 5- Mix with the spoon to blend the aggregates with the added asphalt and transfer them to the mixing bowl
- 6- Turn the mixer on and keep it until the aggregates are completely coated with asphalt (typically 1-1.5 minute).
- 7- Remove the whisk from the mixer and wipe off the fine aggregates using a spatula.
- 8- Transfer the coated mix to a round pan and scrap the mixing bowl to remove the fine aggregates.

#### ***A.4 Aging and Compaction***

- 1- Place the mix in an oven at a temperature higher by 5 degrees than the compaction temperature for 2 hours.
- 2- Make sure that the pressure, the angle and the gyration speed are set to 600 Kpa , 1.25°, and 30 revolutions/sec respectively.
- 3- If the prepared sample is to be compacted for volumetric testing, set the compaction to compact to  $N_{des} = 100$ . If the prepared sample is to be compacted for dynamic modulus , set the compaction to compact to a height = 175 mm.

- 4- Using a thermometer, check the temperature of the mix: If the temperature is higher than 135°C, remove the mix from the oven and leave it at room temperature while monitoring the temperature change. When the temperature of the mix reaches 3 to 4 degrees higher than the compaction temperature remove the mold, scoop, and spatula from the oven. If the temperature is lower than 135°C, heat the mix in the oven for 15 min at a temperature 15° C higher.
- 5- Place a paper at the bottom of the mold and add the asphalt mix in three layer while rodding it with a spatula at the circumference.
- 6- When the whole mix is in the mold, place a paper at the top and center the mold below the ram. Start the software.
- 7- Follow the procedure of the software. When the compaction ends, remove the sample from the compactor.
- 8- After 5 minutes, the sample would have cooled down and ready to be extruded.
- 9- After extrusion, remove the papers from the sample and leave it to cool down to room temperature by placing it in front of a fan.

#### ***A.5 Coring***

- 1- Place the compacted sample at the bottom of the coring stand; make sure to maintain the orientation of the specimen compaction.
- 2- Tighten the screws of the stand so that the sample is centered and restricted from moving.
- 3- Turn the water on; make sure that the water flow is neither too slow nor too fast.
- 4- Turn the power switch on and rotate the arm until it slightly touches the sample.
- 5- Make sure that the break of the coring arm is opened to the max.

- 6- Grab the coring machine arm without applying any force and allow the coring process to take place.
- 7- When the arm reaches the bottom of the sample, pull out the coring arm slowly and turn the machine off.
- 8- Loosen the screws and remove the sample. Make sure to mark the top of the cored sample.

#### ***A.6 Sawing***

- 1- Fill the saw reservoir with water to cover the pump
- 2- Mark 14mm from the top of the sample, place it on the jig and make sure that the saw blade cuts from inside of the sample.
- 3- Secure the sample in its place and turn the saw and the water pump on
- 4- Very slowly pull down the saw to cut the specimen. Make sure to move slowly so as not to damage the bottom of the specimen.
- 5- Turn the saw off.
- 6- Move the jig to the left side of the saw and mark from the cut end of the specimen to the saw 150mm to cut the sample to that exact height.

#### ***A.7 Gluing Specimens***

1. Clean the end plates of the gluing stand and the sides where the targets are to be glued with acetone.
2. Make sure to glue the target on a place where there is no clear air void on the surface or a large sized aggregate.
3. Use Devcon glue to glue the targets; make sure to mix the two liquids very well.
4. Leave the glue to harden for 4 hours at least before fixing the brackets on.

## APPENDIX – B

### PHOTOGRAPHS

#### *B.1 Raw Material*



B. 1 Natural limestone aggregates used



B. 2 Recycled aggregates used





B. 3 Asphalt cans filled and prepared to be used in mixing



B. 4 Sample of Batched Material





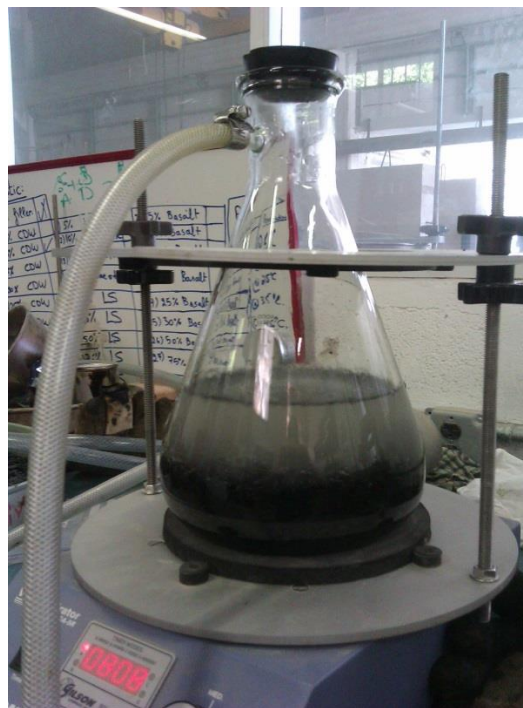
B. 5 Sample mixing



B. 6 Asphalt sample compacted using Superpave Gyrotory Compactor.



B. 7 Sample submerged in water to measure  $G_{mb}$



B. 8 Sample being tested to calculate  $G_{mm}$





B. 9 Sample being prepared for coring



B. 10 Sample being cored



B. 11 Three phases of the asphalt sample



B. 12 Sample being sawed



B. 13 Sample being glued

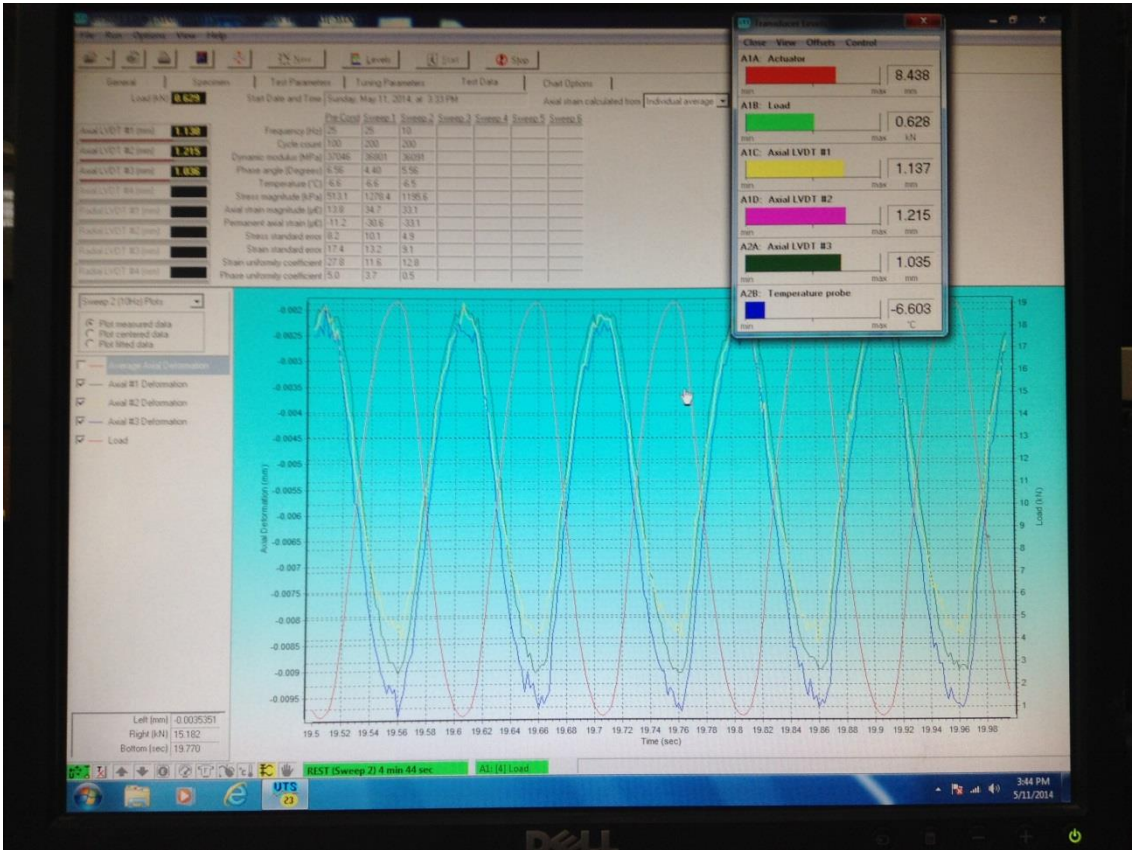




B. 14 Installing brackets



B. 15 Sample conditioning for Dynamic modulus test

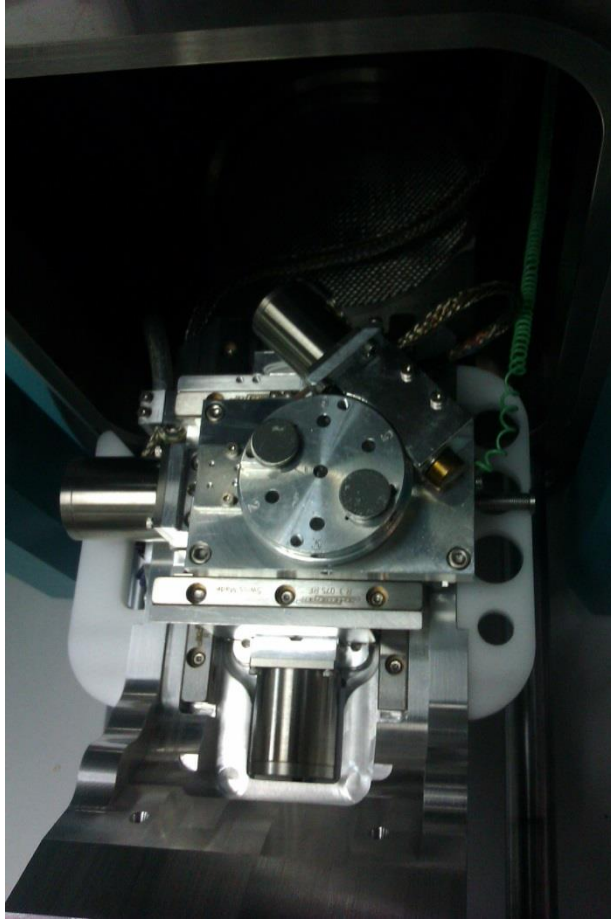


B. 16 Stresses and strains during the dynamic modulus test



B. 17 Scanning Electron Microscope used at the CRSL





B. 18 Aggregates samples placed in the SEM machine



B. 19 BET machine used to measure the surface area of the filler material



B. 20 Mixer used to prepare the mastic (filler + binder)



B. 21 Mastic samples prepared



## APPENDIX-C

### DYNAMIC MODULUS DATA

<b>Specimen Name : XX-YYY-%%-Z- Replicate number</b>	XX: SU for Superpave, MA for Marshall	YYY: Project ID: CDW	%%: CDW replacement %	Z: Test type E for dynamic modulus
--	--	-------------------------	--------------------------	---------------------------------------

SU-CDW-0%-E-1			SU-CDW-0%-E-2			SU-CDW-0%-E-3		
Temp.	Reduced Frequency	Actual E*	Temp.	Reduced Frequency	Actual E*	Temp.	Reduced Frequency	Actual E*
-5	36585519.7	36435.2	-7.1	139147508	35953.3	-7	-	-
	14634207.9	34639.4		69573754.2	35398.1		21773085.86	38647.8
	7317103.95	33782.2		34786877.1	34749.8		10886542.93	36161.5
	1463420.79	32051.5		6957375.42	32949.4		2177308.586	34268.9
	731710.395	30537.5		3478687.71	32044.5		1088654.293	33448.1
	146342.079	29076.1		695737.542	29520.0		217730.8586	30335.4
10	7360.17143	22665.6	9.9	69573.7542	25761.0	10	21773.08586	26144.3
	2944.06857	20292.5		8418.71354	21485.2		10261.58594	23925.0
	1472.03429	18819.2		4209.35677	19911.4		5130.792969	22727.6
	294.406857	15028.1		2104.67838	18535.4		2565.396484	21043.5
	147.203429	13589.9		420.935677	15057.4		513.0792969	17773.0
	29.4406857	9963.9		210.467838	13870.3		256.5396484	16279.8
25	25	9819.6	25	42.0935677	10479.5	25	51.30792969	12699.9
	10	7659.7		4.20935677	6196.3		5.130792969	8328.7
	5	6223.8		20	8330.2		20	11056.4
	1	3682.7		10	7393.4		10	9608.4
	0.5	2868.8		5	6376.2		5	8123.5
	0.1	1484.3		1	4127.8		1	5067.7
40	0.20855988	2259.4	40	0.5	3357.9	39.9	0.5	4076.3
	0.08342395	1420.0		0.1	1872.6		0.1	2292.3
	0.04171198	1037.0		0.01	689.2		0.01	1058.9
	0.0083424	508.4		0.13914983	2181.4		0.142996744	3403.8
	0.0041712	391.5		0.06957492	1583.8		0.071498372	2499.7
	0.00083424	237.6		0.03478746	1186.4		0.035749186	1830.3
		0.00695749	614.0	0.007149837	1023.1			
		0.00347875	473.1	0.003574919	823.6			
		0.00069575	293.6	0.000714984	386.2			

SU-CDW-10%-E-1			SU-CDW-10%-E-2			SU-CDW-10%-E-3		
Temp.	Reduced Frequency	Actual E*	Temp.	Reduced Frequency	Actual E*	Temp.	Reduced Frequency	Actual E*
-7.5	14031786	35825.4	-6.8	11740672.5	39073.0	-6.9	11740672.5	38291.5
	7015893.2	35149.4		5870336.23	37296.2		5870336.23	36550.31
	3507946.6	34486.0		2935168.12	36439.5		2935168.12	35710.76
	701589.32	32617.9		587033.623	33932.9		587033.623	33254.27
	350794.66	31198.2		293516.812	33430.4		293516.812	32761.76
	70158.932	28903.7		58703.3623	30788.3		58703.3623	30172.51
	7015.8932	25289.1		5870.33623	26340.5		5870.33623	25813.73
0.1	529767.02	32078.4	-0.2	354803.714	34184.8	0.1	354803.714	33501.12
	264883.51	30298.1		177401.857	33180.3		177401.857	32516.73
	132441.76	29729.7		88700.9284	31623.5		88700.9284	30991.05
	26488.351	27329.3		17740.1857	28713.4		17740.1857	28139.16
	13244.176	25407.7		8870.09284	27399.1		8870.09284	26851.12
	2648.8351	22061.5		1774.01857	23116.2		1774.01857	22653.86
	264.88351	17205.1		177.401857	15835.1		177.401857	15518.38
9.9	8595.4382	26153.4	10	8283.61902	26721.8	10.1	8283.61902	26187.41
	4297.7191	25339.8		4141.80951	24573.8		4141.80951	24082.28
	2148.8595	22970.2		2070.90476	22890.7		2070.90476	22432.92
	429.77191	18328.4		414.180951	18908.1		414.180951	18529.97
	214.88595	16327.5		207.090476	16950.9		207.090476	16611.84
	42.977191	11739.8		41.4180951	12932.9		41.4180951	12674.23
	4.2977191	6481.8		4.14180951	7139.0		4.14180951	6996.176
25	20	10430.1	25	20	10473.5	25	20	10638.71
	10	8723.3		10	9268.7		10	8897.751
	5	7150.0		5	7776.9		5	7293.024
	1	4324.9		1	4716.4		1	4411.352
	0.5	3589.6		0.5	4085.6		0.5	3661.424
	0.1	1735.9		0.1	1999.2		0.1	1770.589
	0.01	871.9		0.01	1028.7		0.01	889.3089
40	0.0632456	2883.5	39.9	0.07479372	2077.9	40.1	0.06324555	
	0.0316228	2218.2		0.03739686	1579.8		0.03162278	
	0.0158114	1629.5		0.01869843	1210.5		0.01581139	1662.053
	0.0031623	759.2		0.00373969	623.2		0.00316228	774.3739
	0.0015811	644.5		0.00186984	475.0		0.00158114	657.3541
	0.0003162	422.7		0.00037397	267.9		0.00031623	431.1322

SU-CDW-15%-E-1			SU-CDW-15%-E-2			SU-CDW-15%-E-3				
Temp.	Reduced Frequency	Actual E*	Temp.	Reduced Frequency	Actual E*	Temp.	Reduced Frequency	Actual E*		
-7.1	5864542.5	35810.0	-6.8	13687632	38756.64	-6.9	13687632	39919.34		
	2932271.3	35020.2		6843816.1	36517.45		6843816.1	37612.97		
	1466135.6	34560.4		3421908.1	36203.51		3421908.1	37289.62		
	293227.13	32181.9		684381.61	34110.75		684381.61	35134.08		
	146613.56	31010.4		342190.81	32788.71		342190.81	33772.37		
	29322.713	28302.5		68438.161	29952.22		68438.161	30850.78		
10.5	10953.65	25490.78	0.3	6843.8161	25145.95	0.1	6843.8161	25900.33		
	5476.8248	24046.9		637588.53	34792.46		637588.53	35836.24		
	2738.4124	22534.56		318794.26	33242.61		318794.26	34239.89		
	547.68248	18728.16		159397.13	31535.59		159397.13	32481.66		
	273.84124	17097.89		31879.426	29394.63		31879.426	30276.47		
	54.768248	13418.79		15939.713	26987.96		15939.713	27797.59		
	5.4768248	8257.408		3187.9426	23627.57		3187.9426	24336.4		
25	20	11936.99	10.7	318.79426	16731.49	10.2	318.79426	17233.43		
	10	10245.06		18497.289	26677.12		18497.289	27477.43		
	5	8544.953		9248.6446	24847.09		9248.6446	25592.5		
	1	5677.479		4624.3223	23252.46		4624.3223	23950.03		
	0.5	4618.278		924.86446	19514.94		924.86446	20100.39		
	0.1	3285.58		462.43223	17853.3		462.43223	18388.9		
	0.01	2058.698		92.486446	15208.42		100.48645	15664.67		
39.8	0.0115641	1911.73	25	9.2486446	9077.033	25	9.2486446	9349.344		
	0.005782	1559.385		20	11133.77		20	11811.81		
	0.002891	1178.584		10	9447.224		10	10022.56		
	0.0005782	681.7978		5	7775.881		5	8249.432		
	0.0002891	554.3149		1	4717.026		1	5004.293		
	5.782E-05	306.1658		0.5	4131.541		0.5	4383.152		
				0.1	1942.356		0.1	2135.646		
				0.01	875.491		0.01	928.8084		
				39.9	0.0632456		3138.585	40.1	0.0632456	3232.743
					0.0316228		2339.41		0.0316228	2409.593
					0.0158114		1692.087		0.0158114	1742.849
		0.0031623	993.7661		0.0031623	1023.579				
		0.0015811	796.4639		0.0015811	820.3578				
			0.0003162	501.6196		0.0003162	516.6682			

SU-CDW-20%-E-1			SU-CDW-20%-E-2			SU-CDW-20%-E-3		
Temp.	Reduced Frequency	Actual E*	Temp.	Reduced Frequency	Actual E*	Temp.	Reduced Frequency	Actual E*
-7	23405426	35523.2	-7	9331163.6	35838.5	-6.9	9331163.65	36233.6
	11702713	34257.5		4665581.8	35417.1		4665581.82	34942.7
	5851356.6	34091.7		2332790.9	34441.6		2332790.91	34773.6
	1170271.3	31969.7		466558.18	32836.5		466558.182	32609.1
	585135.66	31170.7		233279.09	31979.5		233279.091	31794.1
	117027.13	28805.1		46655.818	29146.8		46655.8182	29381.3
	11702.713	24640.6		4665.5818	24925.4		4682.582	25133.4
9.9	6819.9549	23323.6	10.1	3738.0821	24987.0	9.9	3738.08207	23790.1
	3409.9774	21709.9		1869.041	22890.5		1869.04103	22144.1
	1704.9887	20440.0		934.52052	20588.7		934.520517	20848.8
	340.99774	17206.9		186.9041	16884.1		186.904103	17551.0
	170.49887	15551.5		93.452052	15079.1		93.4520517	15862.5
	34.099774	11839.5		18.69041	11055.5		21.69041	11714.0
	3.4099774	7010.6		1.869041	5577.7		1.86904103	6578.7
25	20	10338.9	25	20	10636.9	25	20	10338.9
	10	9022.2		10	9066.4		10	9022.2
	5	7776.0		5	7588.8		5	7776.0
	1	5248.8		1	5072.8		1	5248.8
	0.5	4322.7		0.5	4169.9		0.5	4322.7
	0.1	2504.8		0.1	2690.0		0.1	2504.8
	0.01	1333.8		0.01	1181.6		0.01	1333.8
39.9	0.1259553	3056.0	40	0.0892154	2525.8	39.9	0.12595534	3056.0
	0.0629777	2382.2		0.0446077	1948.2		0.06297767	2382.2
	0.0314888	1806.4		0.0223039	1472.2		0.03148883	1806.4
	0.0062978	1016.8		0.0044608	833.4		0.00629777	1016.8
	0.0031489	792.6		0.0022304	656.9		0.00314888	792.6
	0.0006298	521.4		0.0004461	348.0		0.00062978	521.4

SU-CDW-30%-E-1			SU-CDW-30%-E-2			SU-CDW-30%-E-3		
Temp.	Reduced Frequency	Actual E*	Temp.	Reduced Frequency	Actual E*	Temp.	Reduced Frequency	Actual E*
-6.8	37730849	32293.3	-7.5	11799986.5	31484.1	-7.1	37730849.2	32293.26
	18865425	31500.3		5899993.27	30218.2		18865424.6	31500.3
	9432712.3	31333.6		2949996.64	30155.3		9432712.3	31333.63
	1886542.5	29594.1		589999.327	28361.5		1886542.46	29594.11
	943271.23	28636.6		294999.664	27671.2		943271.23	28636.62
	188654.25	26625.1		58999.9327	25619.6		188654.246	26625.13
	18865.425	22732.3		5899.99327	21945.7		18865.4246	22732.31
10	4898.1493	20165.6	10.2	4213.38807	21099.1	9.9	4898.14929	20165.57
	2449.0746	18577.7		2106.69404	19507.3		2449.07465	18577.67
	1224.5373	16815.5		1053.34702	18050.5		1224.53732	16815.46
	244.90746	13509.6		210.669404	14514.1		244.907465	13509.56
	122.45373	11955.7		105.334702	12862.7		122.453732	11955.71
	24.490746	8760.8		21.0669404	9412.1		24.4907465	8760.85
	2.4490746	4919.2		2.10669404	4768.7		2.44907465	4919.244
25	20	8393.4	25	20	9090.7	25	20	8393.429
	10	7230.5		10	7702.7		10	7230.484
	5	6017.1		5	6316.8		5	6017.106
	1	3762.7		1	3867.0		1	3762.658
	0.5	2985.8		0.5	3018.0		0.5	2985.849
	0.1	1629.1		0.1	1624.7		0.1	1629.12
	0.01	763.1		0.01	840.6		0.01	763.149
40	0.231301	2299.8	39.9	0.12907434	1939.7	40.1	0.23130101	1939.67
	0.1156505	1818.2		0.06453717	1544.1		0.1156505	1544.106
	0.0578253	1420.4		0.03226859	1137.2		0.05782525	1137.158
	0.0115651	789.5		0.00645372	665.1		0.01156505	665.09
	0.0057825	616.4		0.00322686	539.9		0.00578253	539.9479
	0.0011565	321.7		0.00064537	307.8		0.00115651	307.8036

